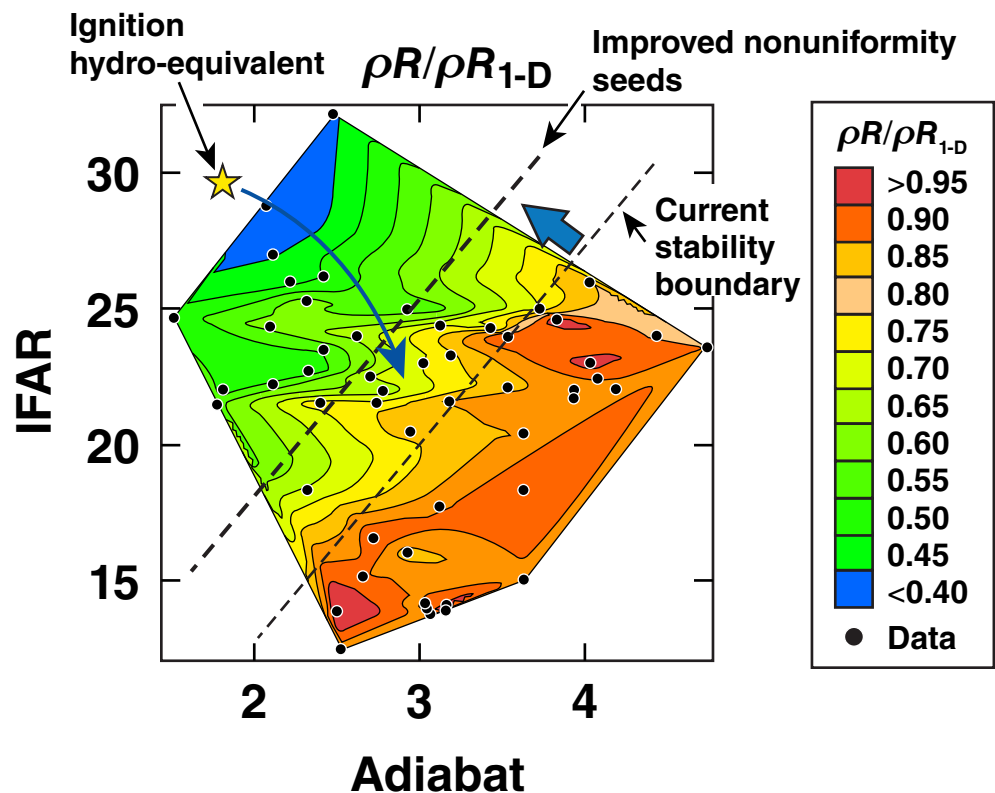
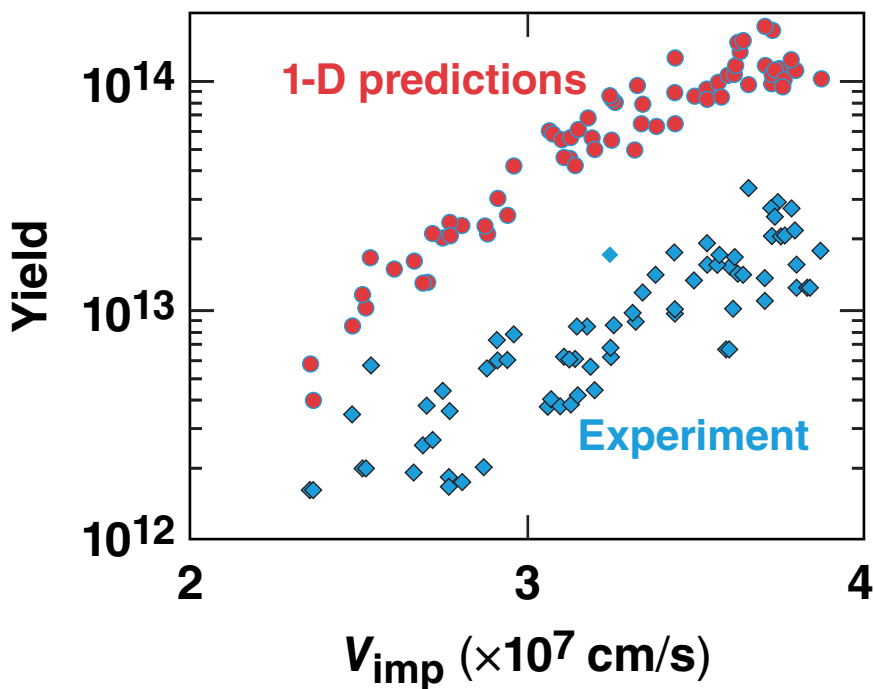


# Demonstrating Ignition Hydrodynamic Equivalence in Cryogenic DT Implosions on OMEGA



V. N. Goncharov  
University of Rochester  
Laboratory for Laser Energetics

55th Annual Meeting of the  
American Physical Society  
Division of Plasma Physics  
Denver, CO  
11–15 November 2013

# The perturbation degradation of OMEGA cryogenic implosions is understood in terms of unshocked shell mass at stagnation



- Yields in excess of  $3.4 \times 10^{13}$  [yield-over-clean (YOC) ~ 35%] and ion temperatures up to 4 keV were measured in cryogenic implosions with  $V_{\text{imp}} \sim 3.8 \times 10^7$  cm/s
- Performance degradation in moderate-adiabat ( $\alpha \sim 4$ ) implosions is fully understood by 2-D DRACO simulations
- Shells in lower-adiabat implosions ( $\alpha \sim 2.5$ ) break up during acceleration, leading to an increased hot-spot mass and reduced convergence
- The unshocked mass at peak compression determines the impact of the ablator mix

Improving shell stability and mitigating cross-beam energy transfer (CBET) are required to demonstrate ignition hydrodynamic scaling on OMEGA.

# Collaborators

---



**T. C. Sangster, R. Betti, T. R. Boehly, T. J. B. Collins,  
R. S. Craxton, J. A. Delettrez, D. H. Edgell, R. Epstein, C. J. Forrest,  
D. H. Froula, V. Yu. Glebov, D. R. Harding, S. X. Hu,  
I. V. Igumenshchev, R. Janezic, J. H. Kelly, T. J. Kessler, T. Z. Kosc,  
S. J. Loucks, J. A. Marozas, F. J. Marshall, A. V. Maximov, R. L.  
McCrory, P. W. McKenty, D. D. Meyerhofer, D. T. Michel,  
J. F. Myatt, R. Nora, P. B. Radha, S. P. Regan, W. Seka, W. T. Shmayda,  
R. W. Short, A. Shvydky, S. Skupsky, C. Sorce, C. Stoeckl,  
and B. Yaakobi**

**Laboratory for Laser Energetics  
University of Rochester**

**J. A. Frenje, M. Gatu Johnson, and R. D. Petrasso  
Plasma Science and Fusion Center, MIT**

**D. T. Casey  
Lawrence Livermore National Laboratory**

# Outline

---



- OMEGA cryogenic target design
- Target performance
- Performance analysis using 2-D DRACO simulations
- Performance degradation mechanisms
- Conclusions

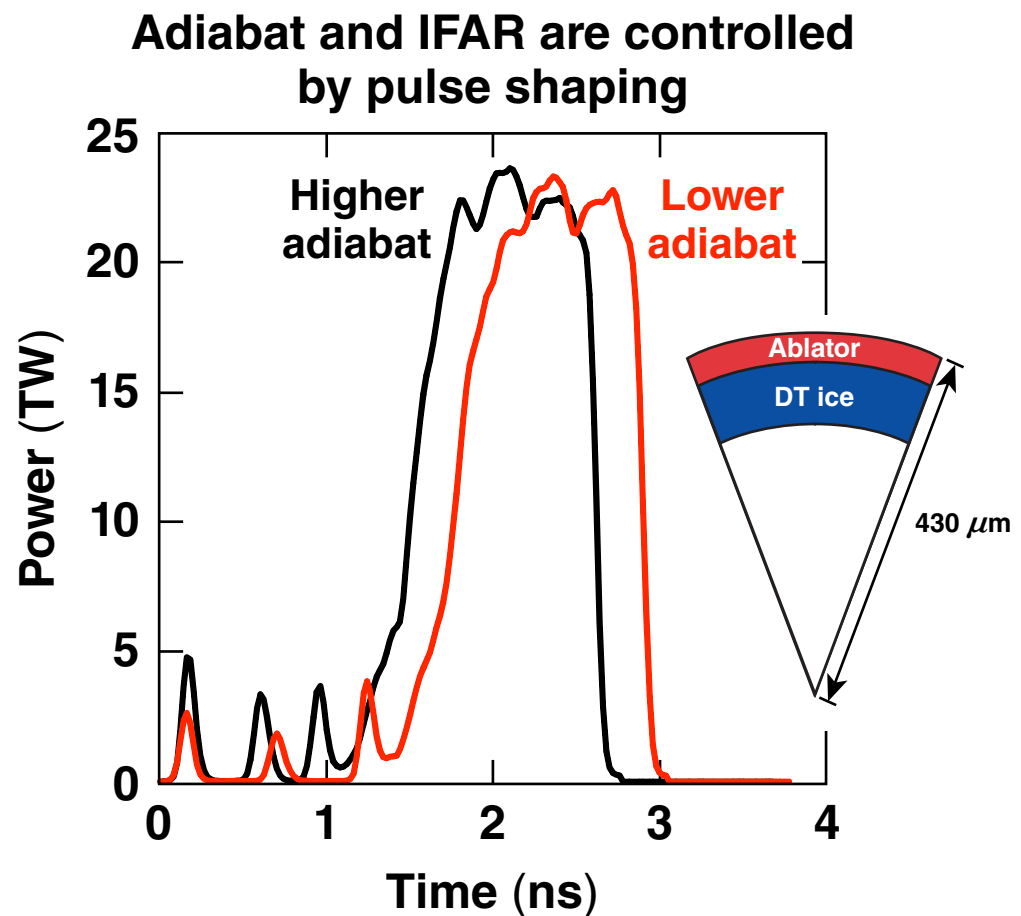
# Direct-drive target performance is optimized by varying implosion velocity, in-flight aspect ratio (IFAR), fuel adiabat, and ablator material



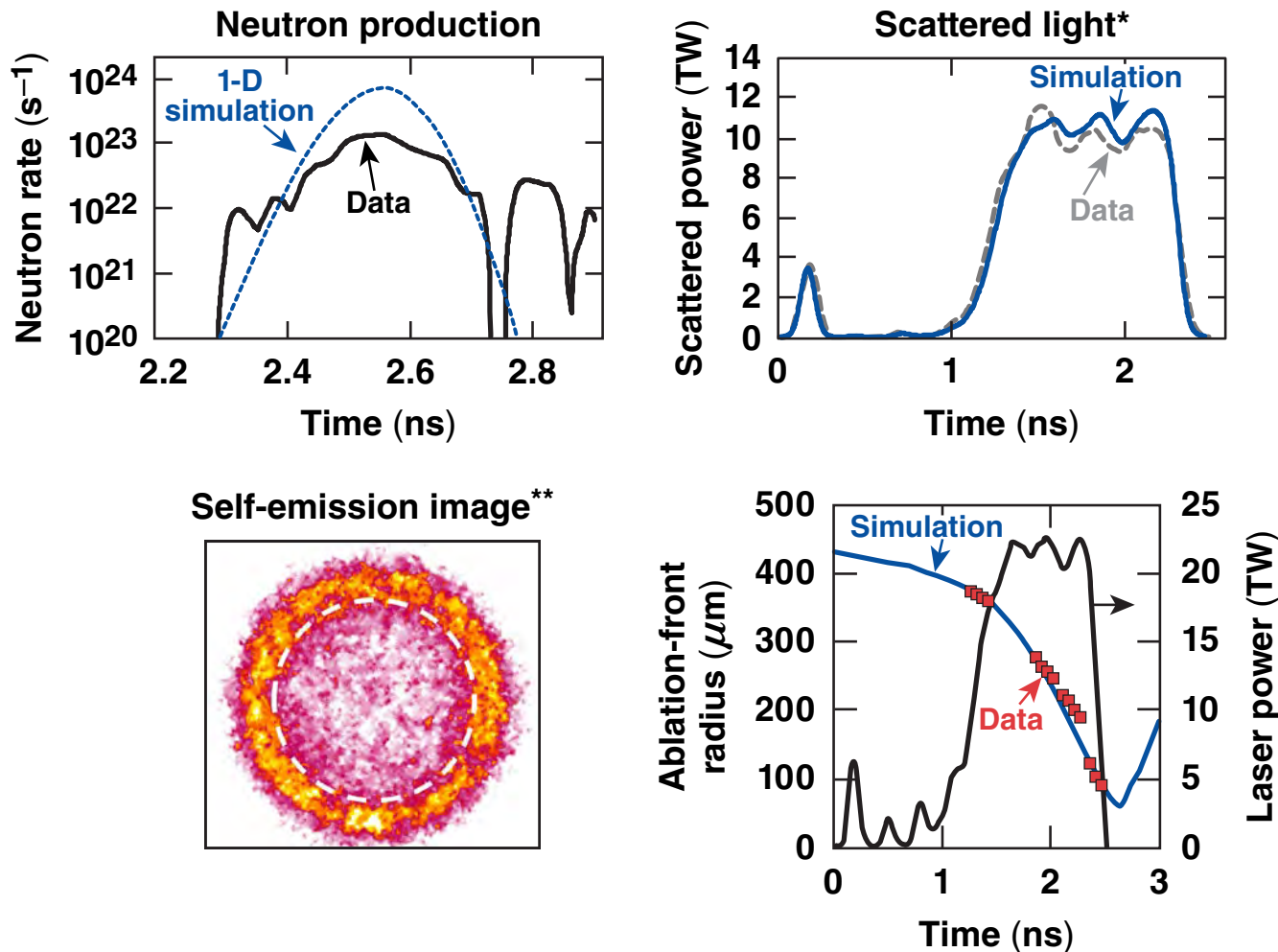
- $V_{\text{imp}}$  and IFAR are controlled by varying the ablator (7.5 to 12  $\mu\text{m}$ ) and fuel thickness (40 to 66  $\mu\text{m}$ )

Adiabat  
 $\alpha = P/P_{\text{Fermi}}$

IFAR = shell radius/  
shell thickness



# One-dimensional dynamics are verified using self-emission, bang time, and scattered-light measurements



\*W. Seka et al., Phys. Plasmas 15, 056312 (2008).

\*\*D. T. Michel et al., N07.00002, this conference.

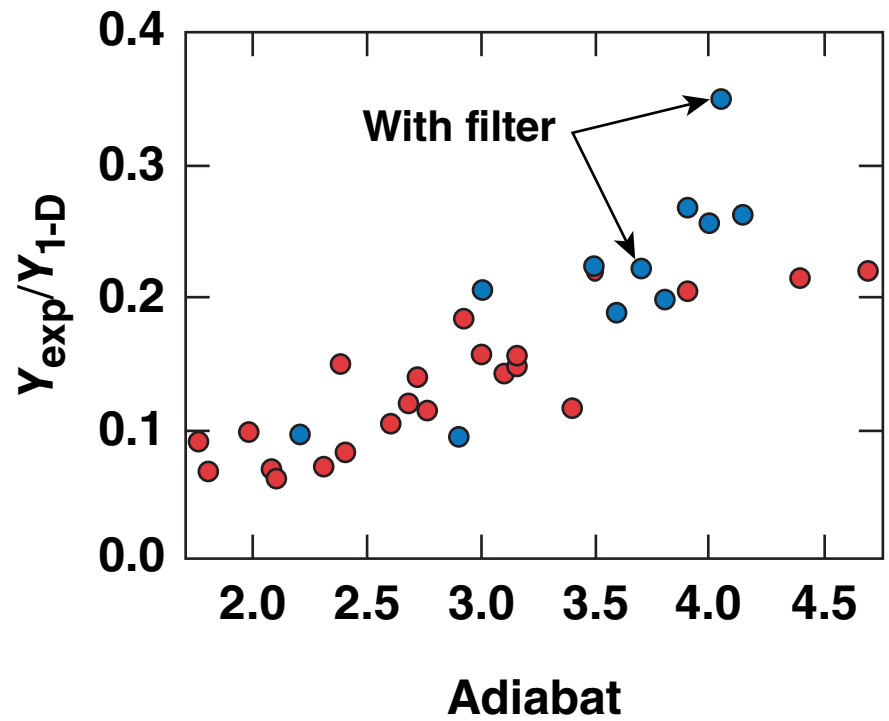
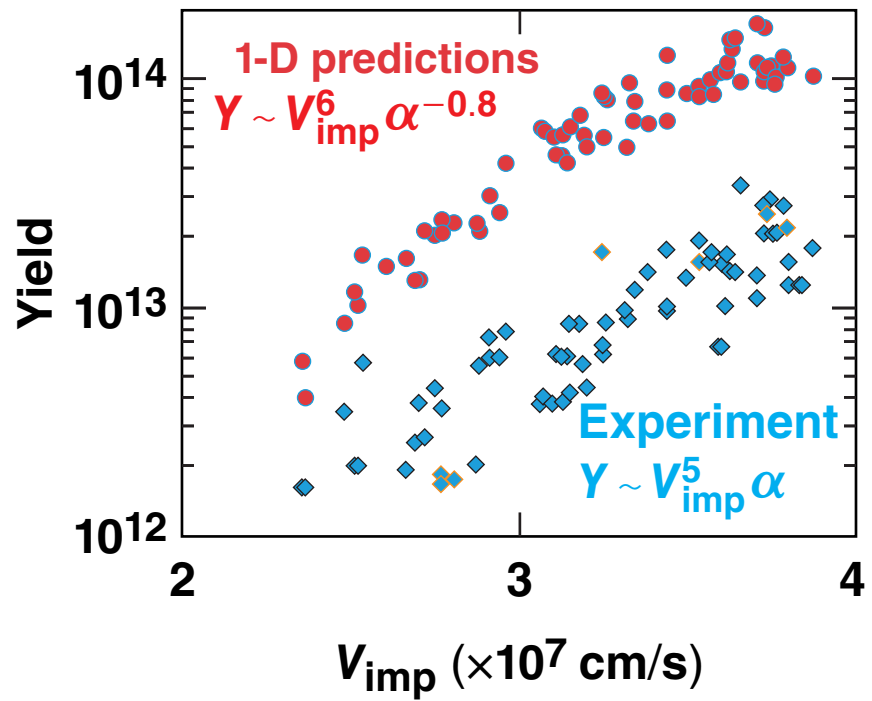
# Outline

---



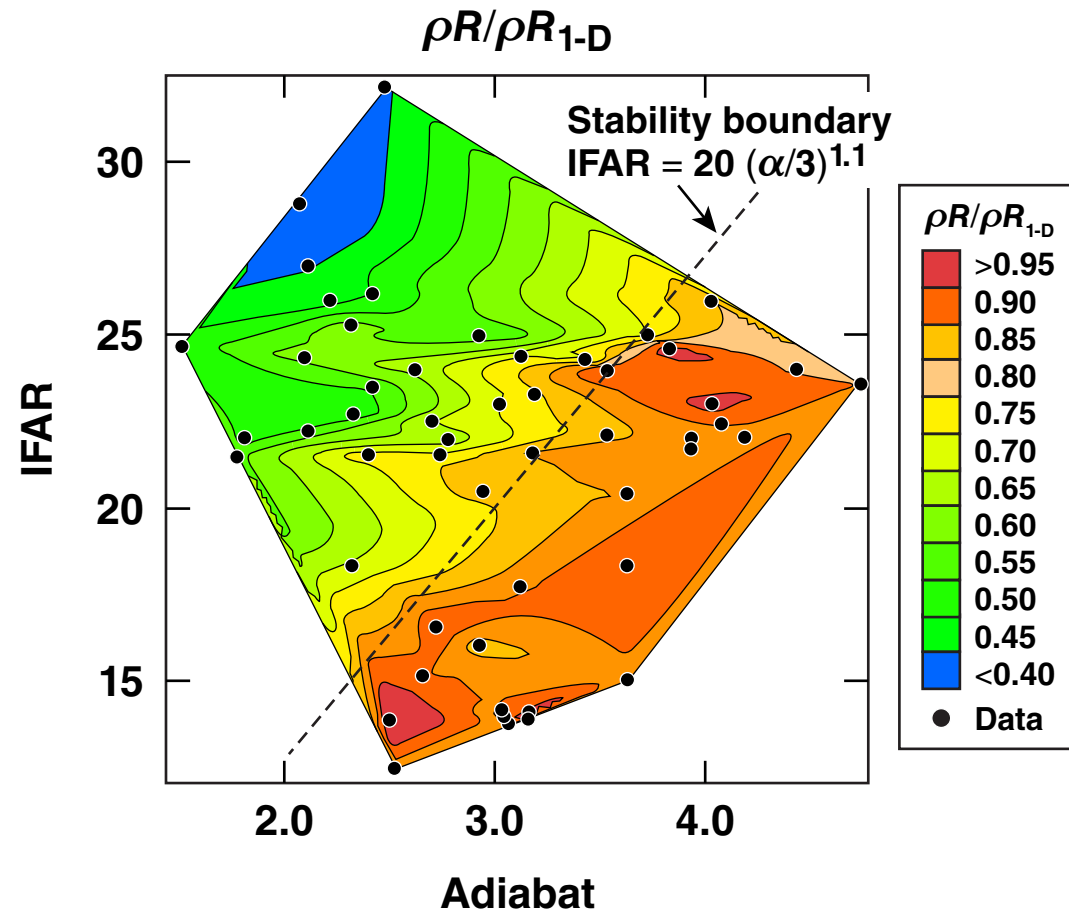
- OMEGA cryogenic target design
- **Target performance**
- Performance analysis using 2-D *DRACO* simulations
- Performance degradation mechanisms
- Conclusions

# Target yield has a strong dependence on implosion velocity



Yields for moderate-adiabat implosions increased by removing non-hydrogen fuel contaminants with a PdAg filter.

# Fuel compression is degraded for low-adiabat, high-IFAR implosions



# The maximum hot-spot pressure can be estimated using the measured neutron production rate

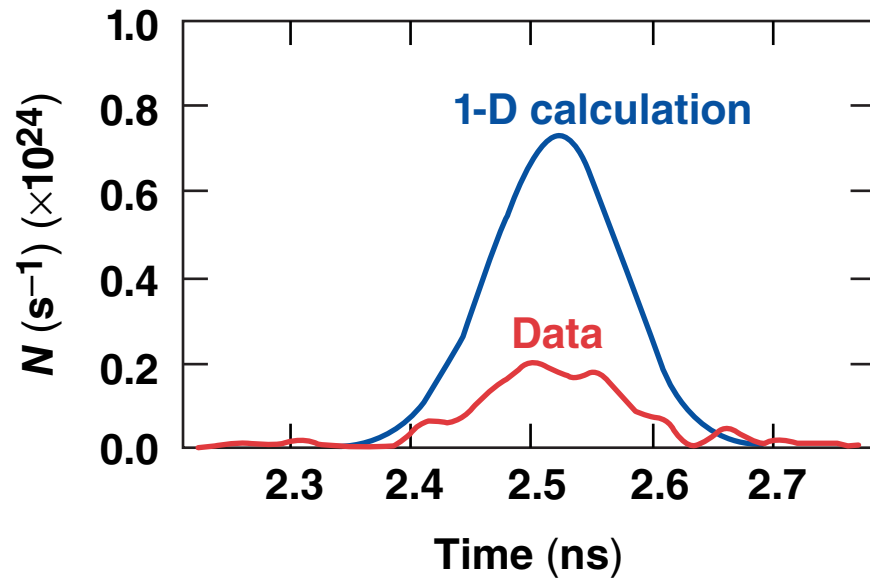
$$\frac{dN}{dt} \sim n^2 \langle \sigma v \rangle V_{hs} \sim p_{hs}^2 V_{hs} T^{2.5}$$

$$p_{hs} V_{hs}^{5/3} = \text{const}$$

$$\frac{dN}{dt} \sim p_{hs}^{7/5} T^{2.5}$$

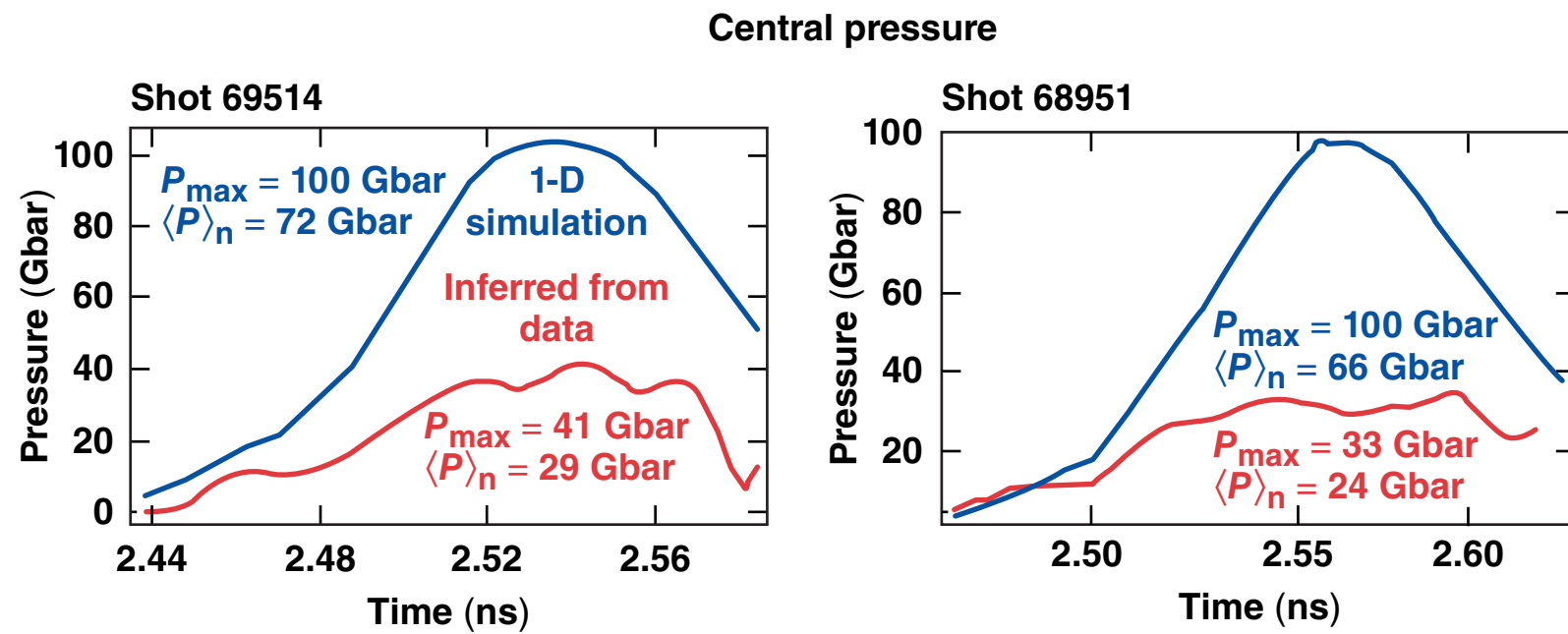
**Measured**

$$p_{exp} \simeq p_{sim} \left( \frac{T_{exp}}{T_{sim}} \right)^{-1.8} \left( \frac{\dot{N}_{exp}}{\dot{N}_{sim}} \right)^{-0.7}$$



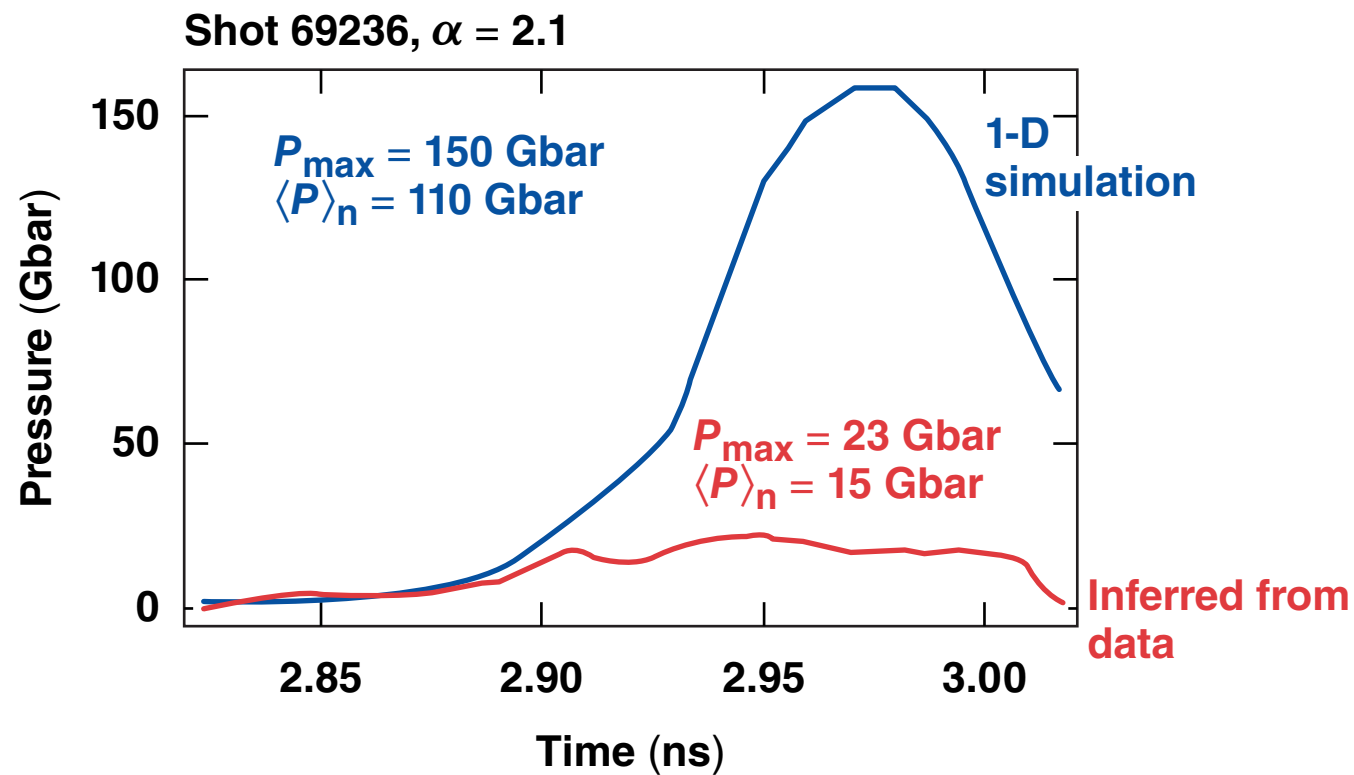
## Target Performance

Pressures up to  $\sim 40$  Gbar are inferred in  $\alpha \sim 4$  implosions



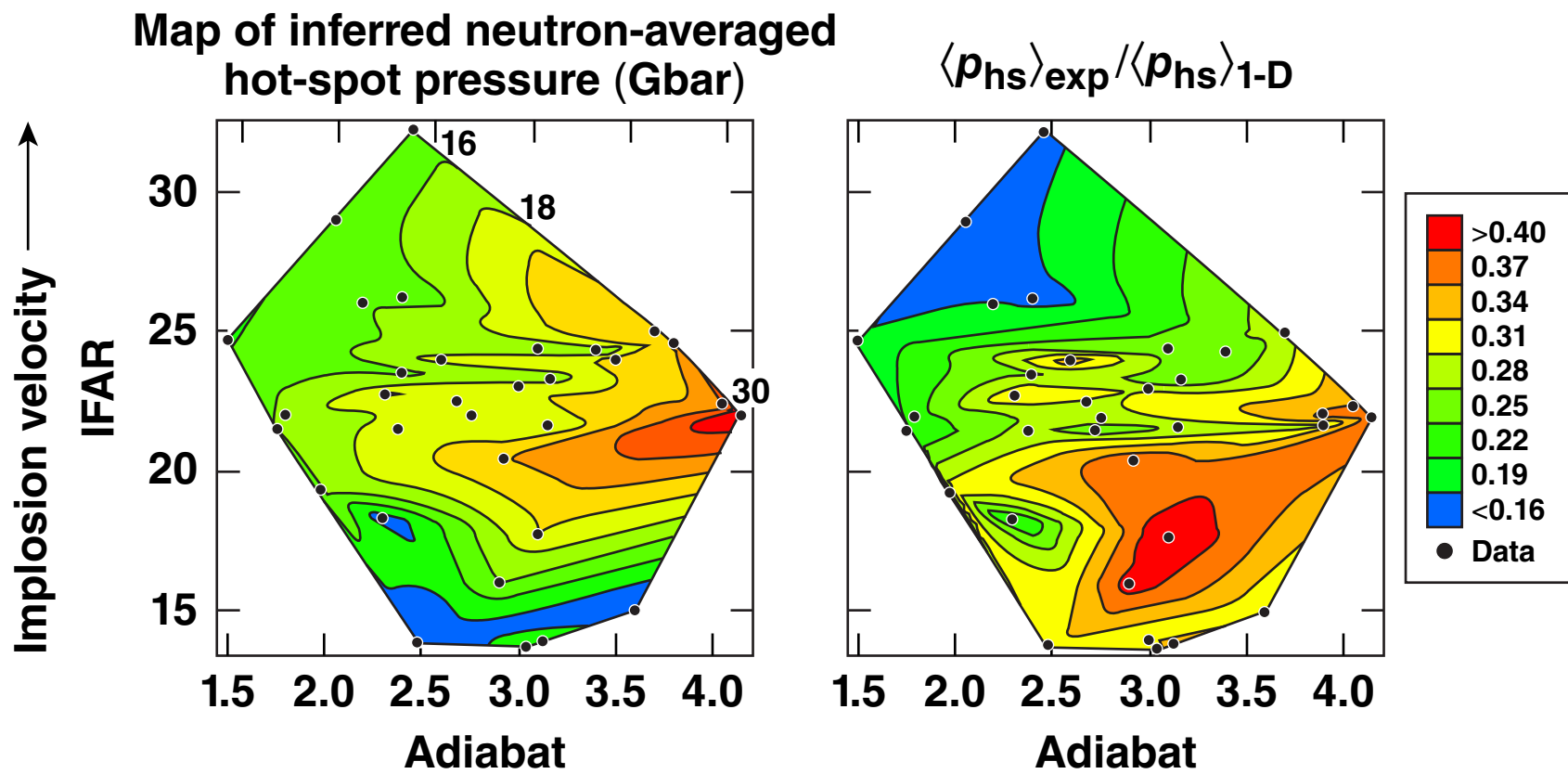
TC10957

# Pressure is significantly reduced in low-adiabat ( $\alpha < 2.5$ ) implosions



## Target Performance

The highest hot-spot pressure is achieved  
for  $\alpha \sim 4$  implosions at IFAR  $\sim 22$



TC10959

# Outline

---



- OMEGA cryogenic target design
- Target performance
- **Performance analysis using 2-D DRACO simulations**
- Performance degradation mechanisms
- Conclusions

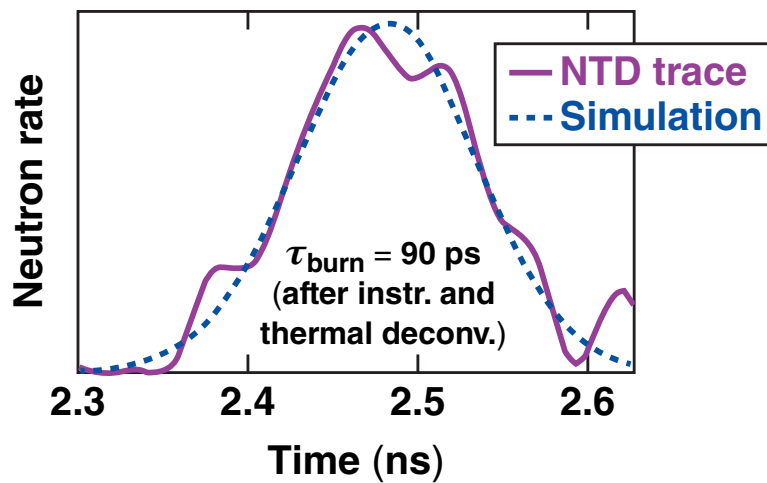
## 2-D Simulations

# Two-dimensional simulations for $\alpha \gtrsim 4$ implosions reproduce measured stagnation quantities\*



- Sources of nonuniformity included in simulation: laser imprint, ice roughness, power imbalance, and beam mistiming

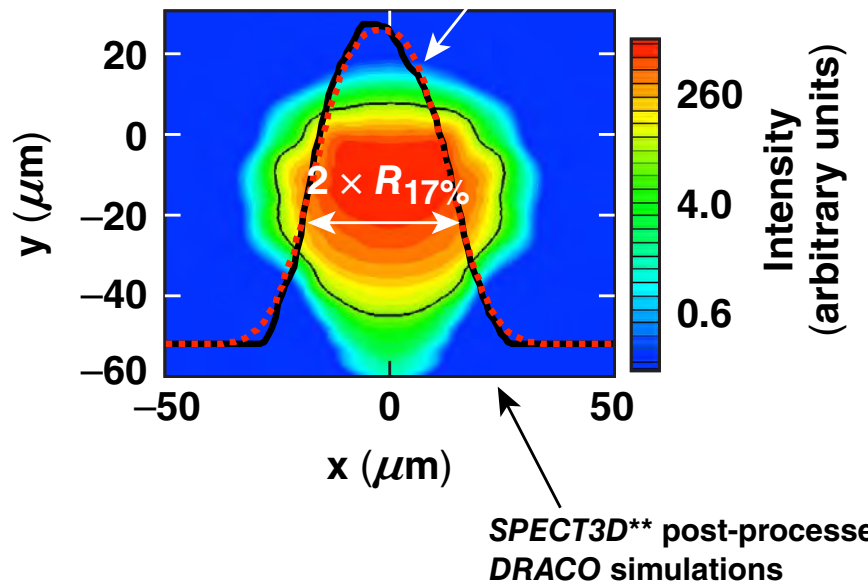
Neutron temporal diagnostic (NTD)  
for shot 69514



	Simulation	Experiment
Yield	$3.9 \times 10^{13}$	$3.0 \times 10^{13}$
$T_i$	3.7 keV	3.6 keV
$\rho R$	0.18 g/cm <sup>2</sup>	0.17 g/cm <sup>2</sup>
$R_{17}$	24.4 $\mu\text{m}$	25.2 $\mu\text{m}$
$P_{\text{hs}}$	32 Gbar	30 Gbar

E22296f

Measured self-emission profile  
for shot 69514



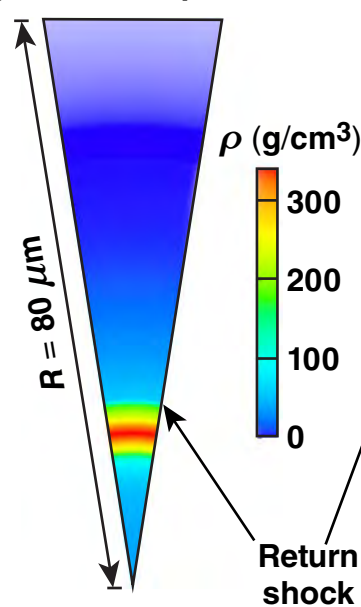
\*S. X. Hu, UO4.00009, this conference.

\*\*Prism Computational Sciences, Inc., Madison, WI, Report PCS-R-025, Ver. 2.1 (2001).

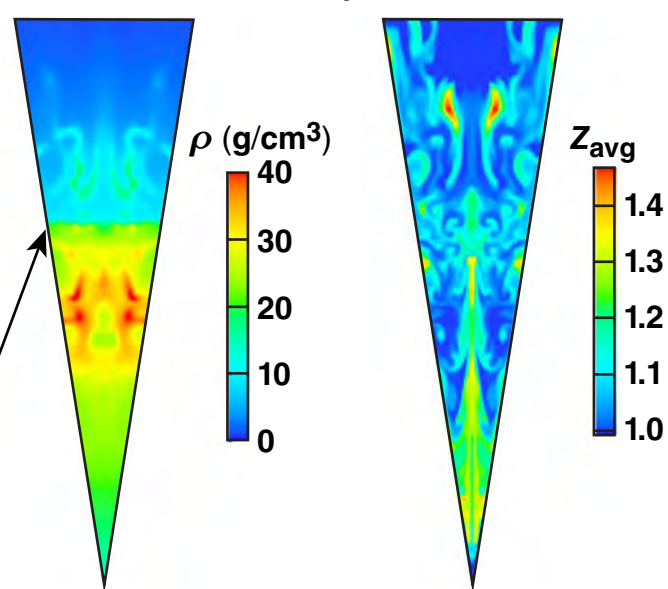
# Shell instability is the main candidate for performance degradation in low-adiabat implosions

- Simulations\* include ~100 surface features, size: 5 to 20  $\mu\text{m}$  in diameter, 0.5 to 1.0  $\mu\text{m}$  in depth

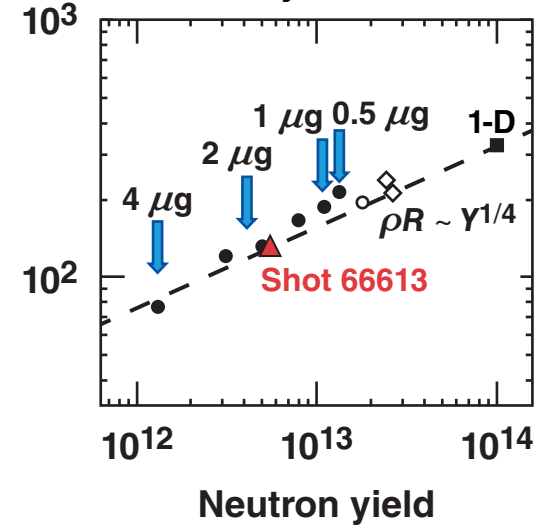
Symmetric implosion



Perturbed implosion



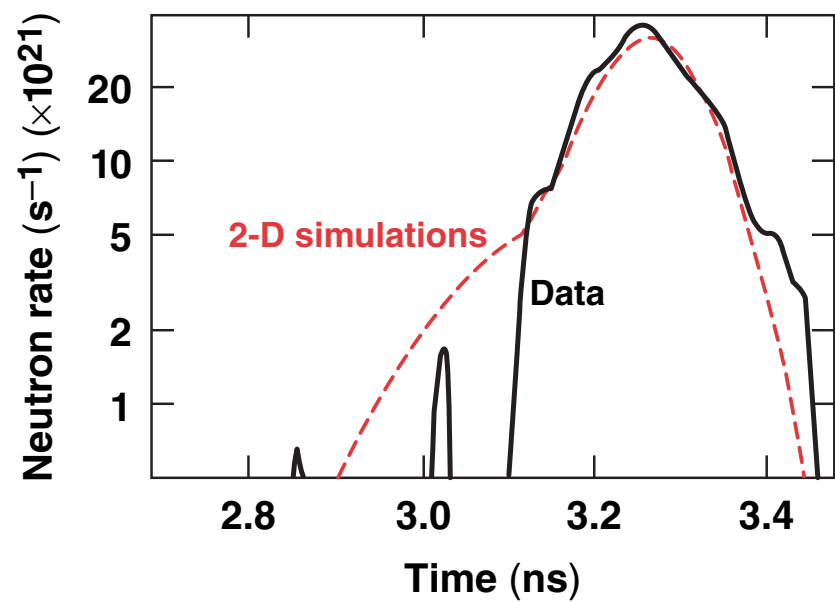
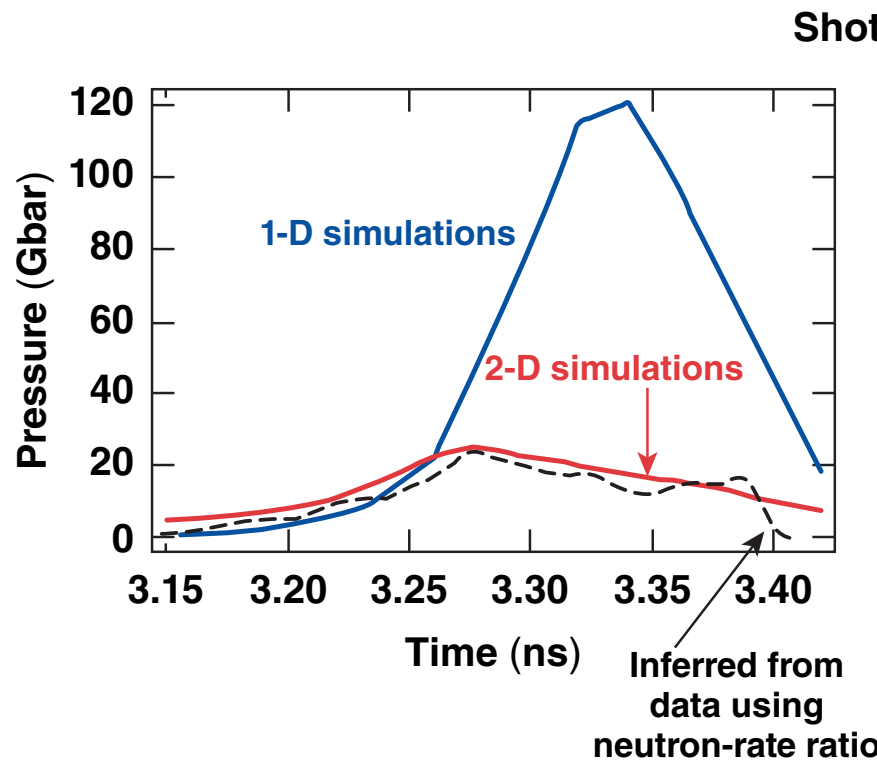
Mass injected into hot spot by mix



The main goal of these simulations is to identify a possible hydrodynamic scenario that explains the observations.

## 2-D Simulations

Hydrodynamic simulations including local defects match the evolution of hot-spot pressure and neutron rate



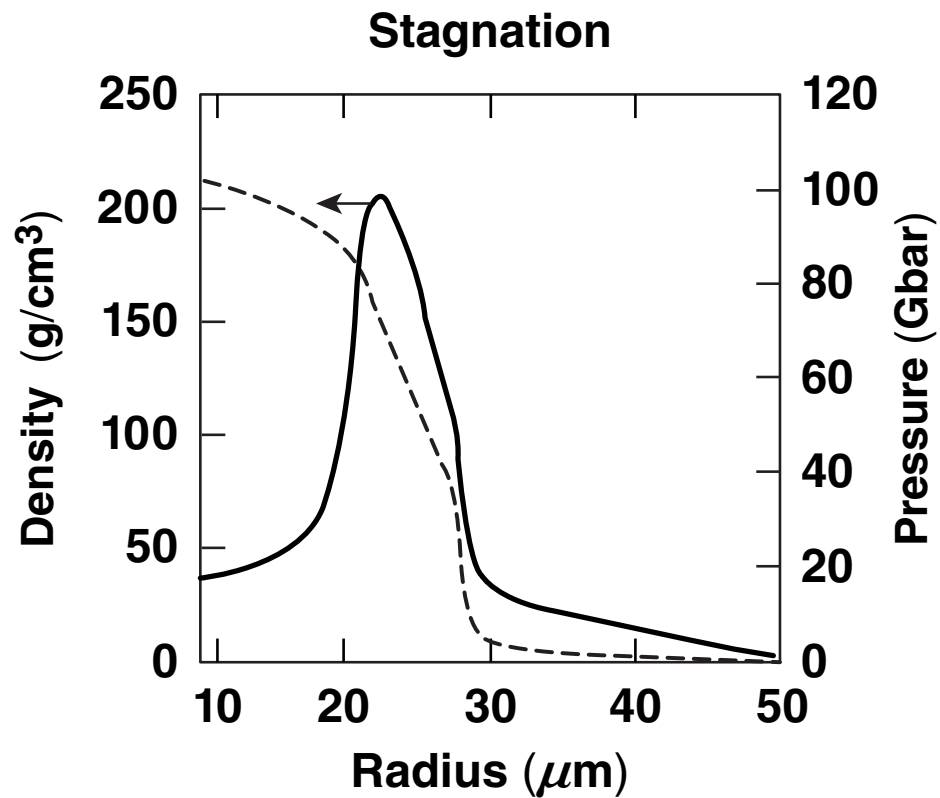
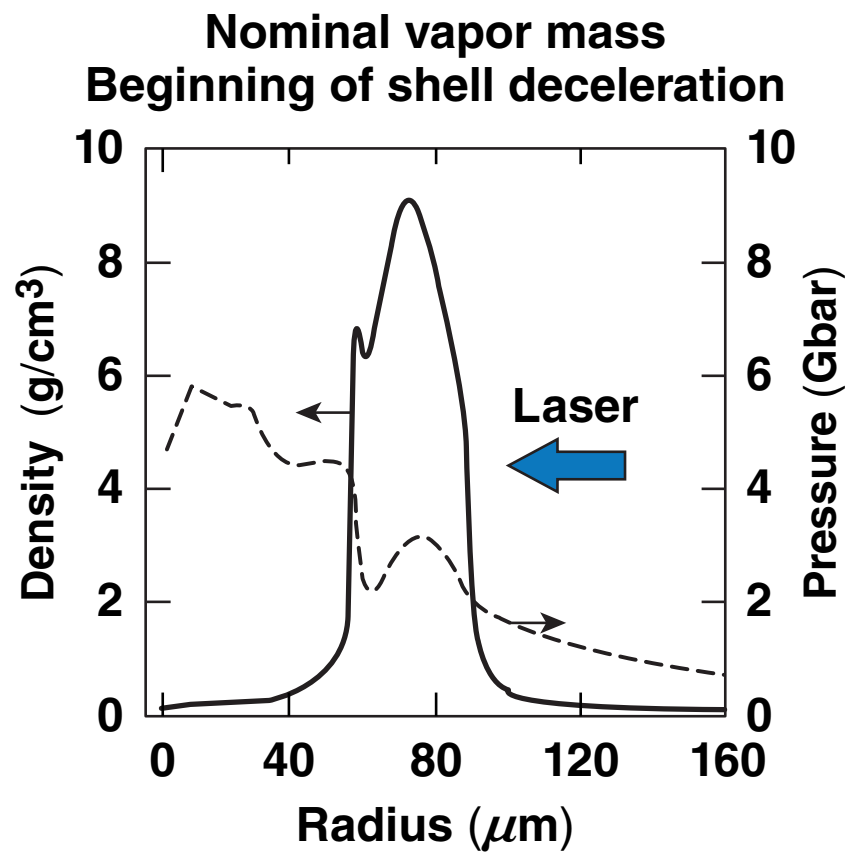
# Outline

---



- OMEGA cryogenic target design
- Target performance
- Performance analysis using 2-D *DRACO* simulations
- **Performance degradation mechanisms**
  - increased vapor mass
  - shell density relaxation caused by Rayleigh–Taylor (RT) mix and preheat
- Conclusions

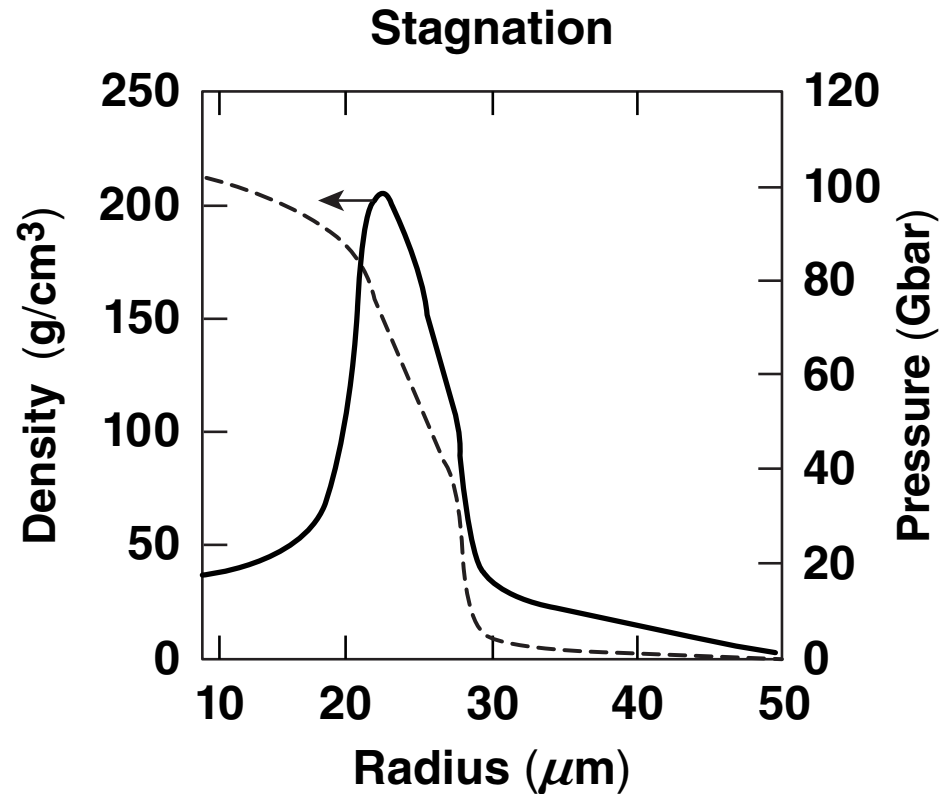
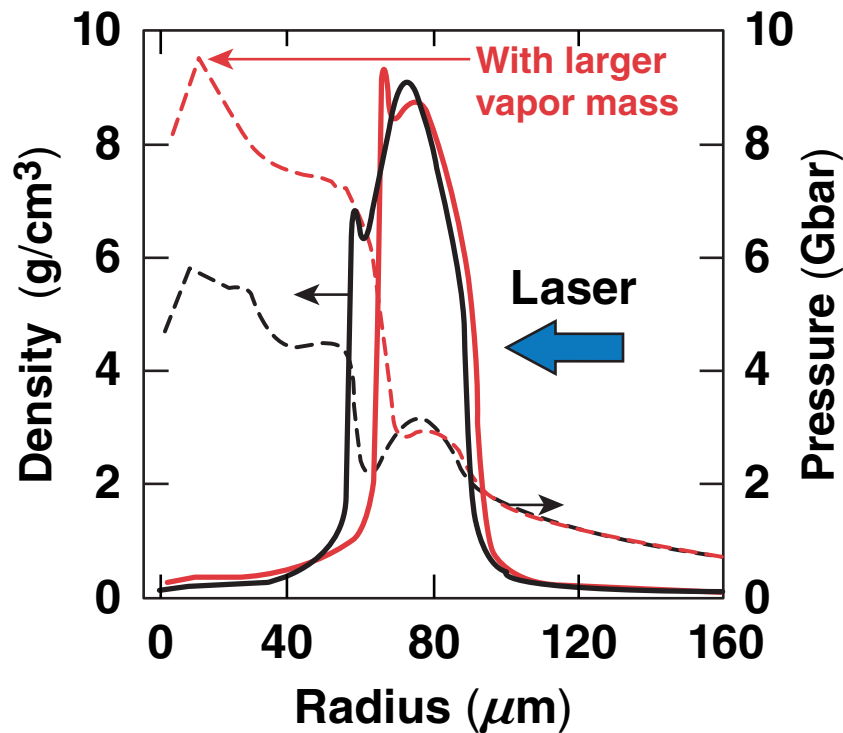
# Excessive vapor mass leads to a larger hot-spot radius at stagnation



# Excessive vapor mass leads to a larger hot-spot radius at stagnation

- Fuel contamination and ablator-to-vapor mix contribute to larger vapor mass

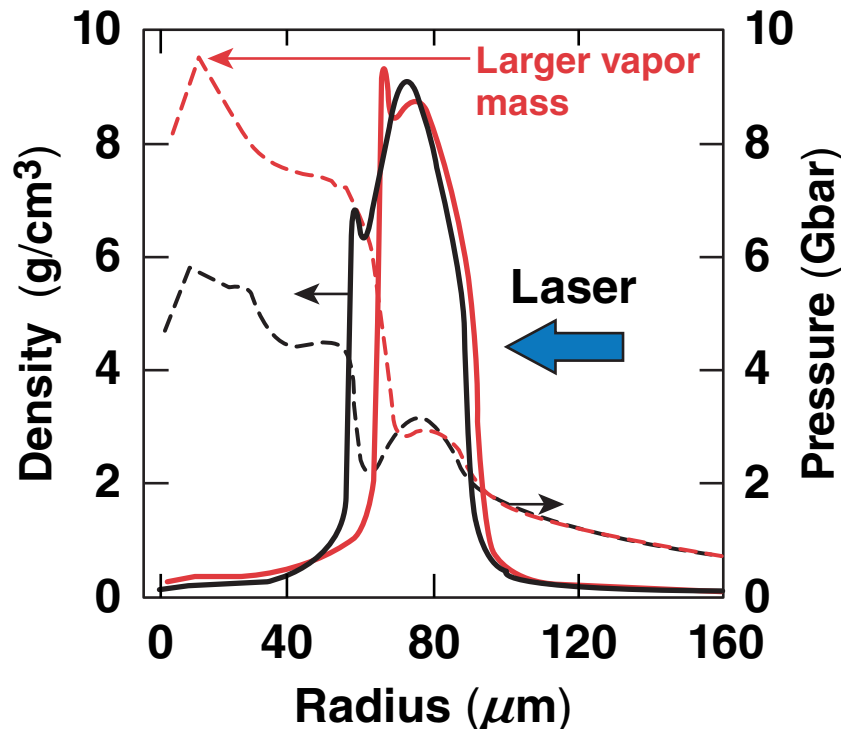
Larger vapor mass leads to stronger shell deceleration



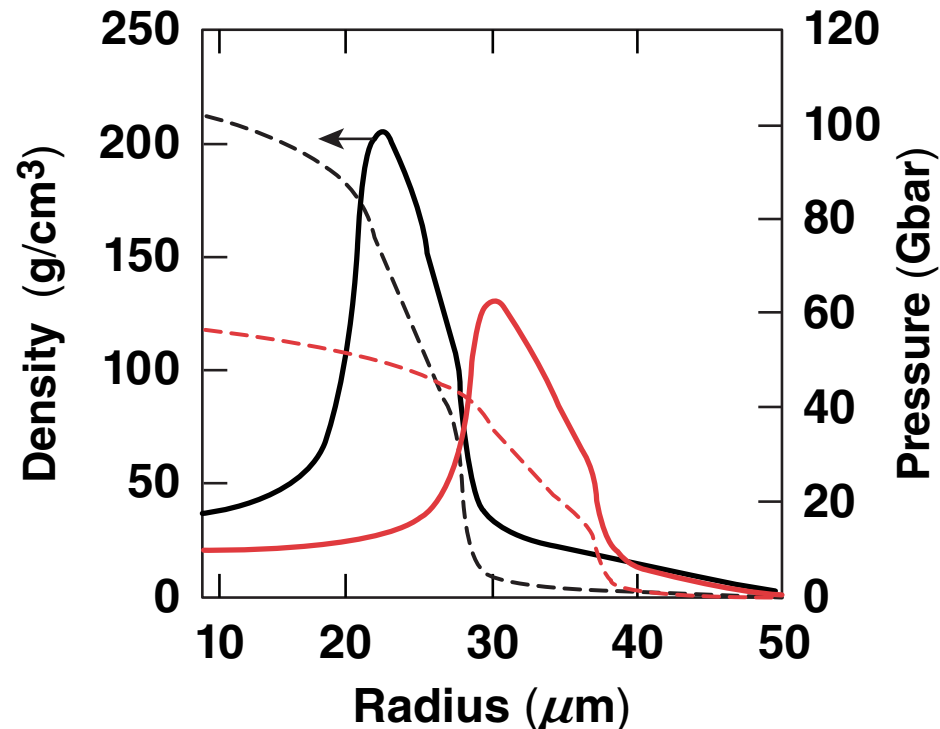
# Excessive vapor mass leads to a larger hot-spot radius at stagnation

- Fuel contamination and ablator-to-vapor mix contribute to larger vapor mass

Larger vapor mass leads to stronger shell deceleration



A shell with more vapor mass stagnates at a larger radius

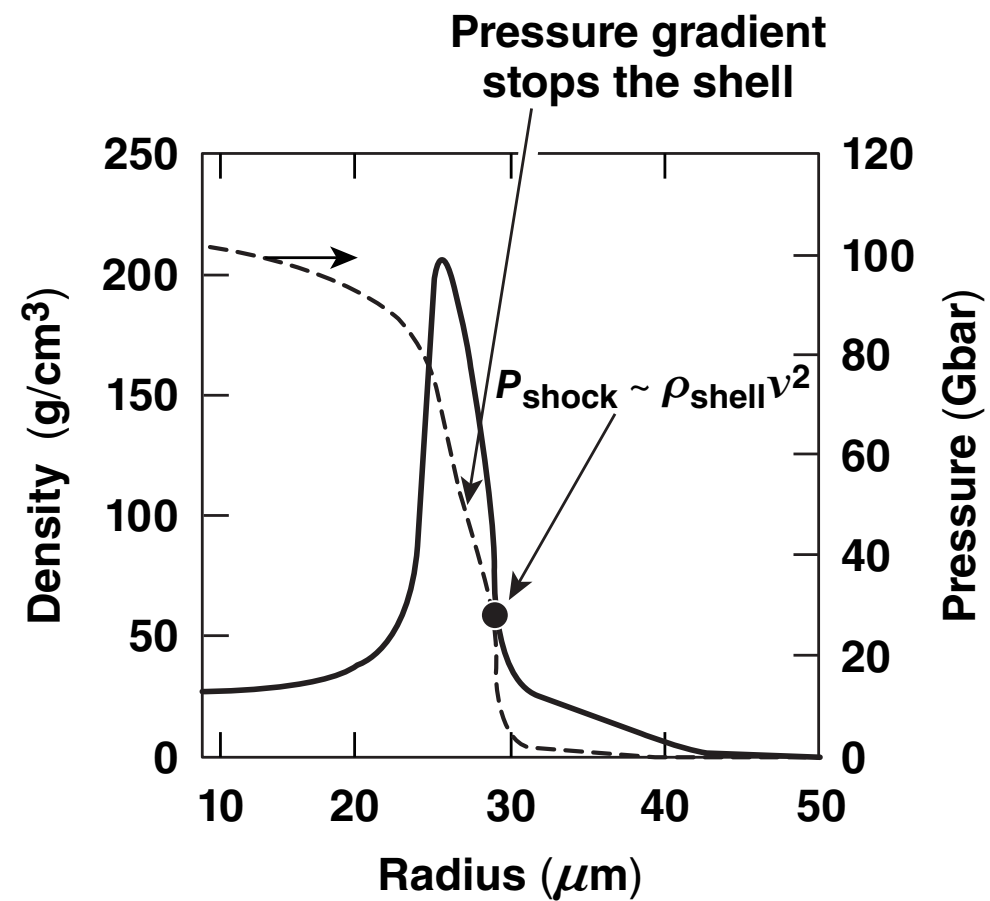
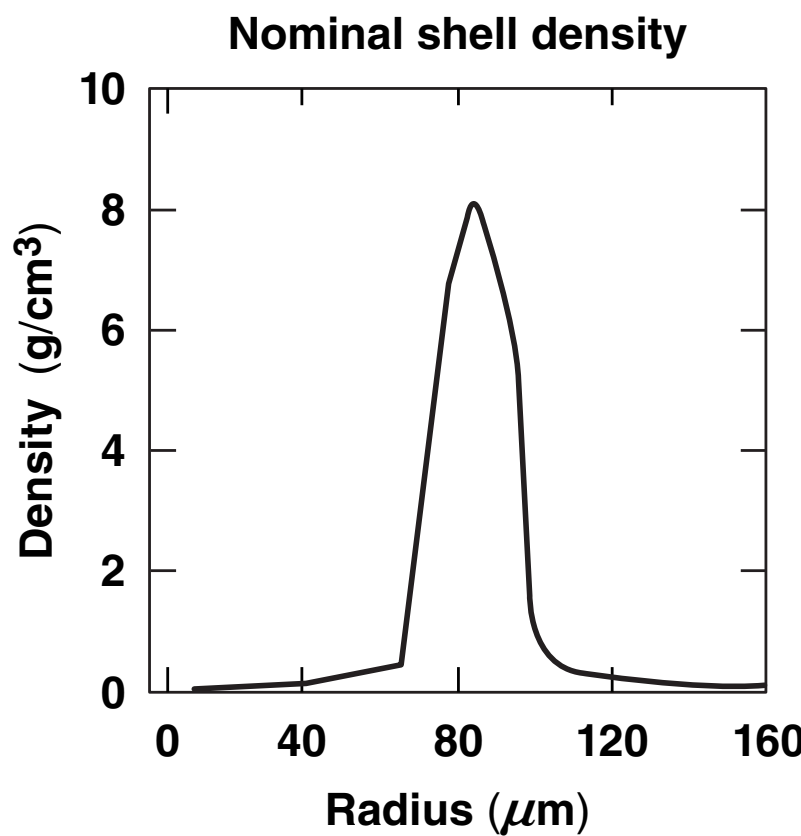


$$\rho R \sim \frac{\rho R_{\max}}{\sqrt{1 + \frac{m_{\text{vapor}}}{m_{\text{norm}}}}}, P_{\text{hs}} \sim \left(1 + \frac{m_{\text{vapor}}}{m_{\text{norm}}}\right)^{0.8}$$

TC10991b

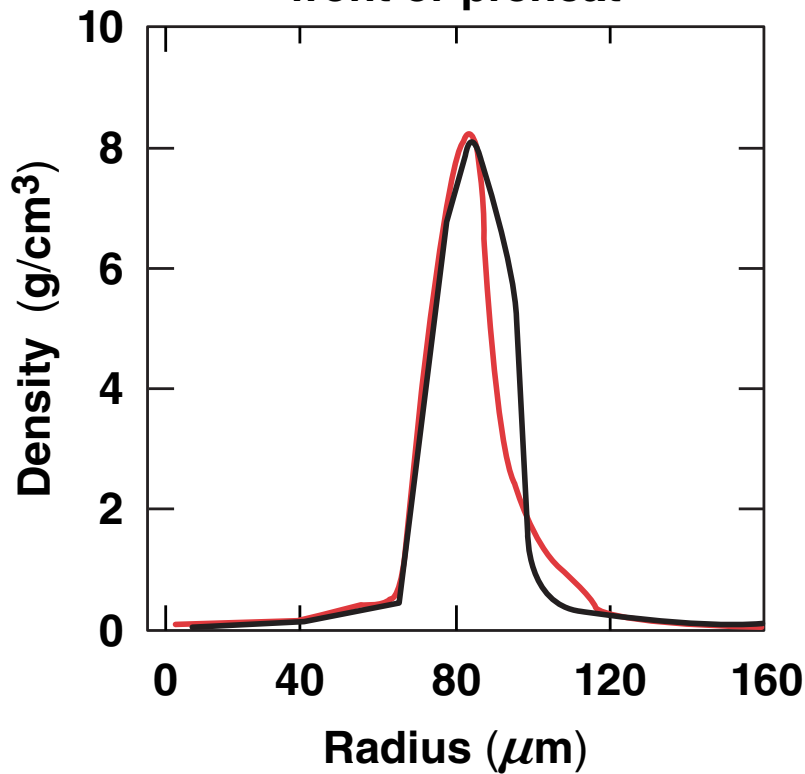
For OMEGA targets:  $m_{\text{norm}} = 0.1 \mu\text{g}$   
Vapor mass increases to  $2 \mu\text{g}$  because of mix in  $\alpha < 2.5$  implosions

# Reduced shell density contributes to degradation in hot-spot compression

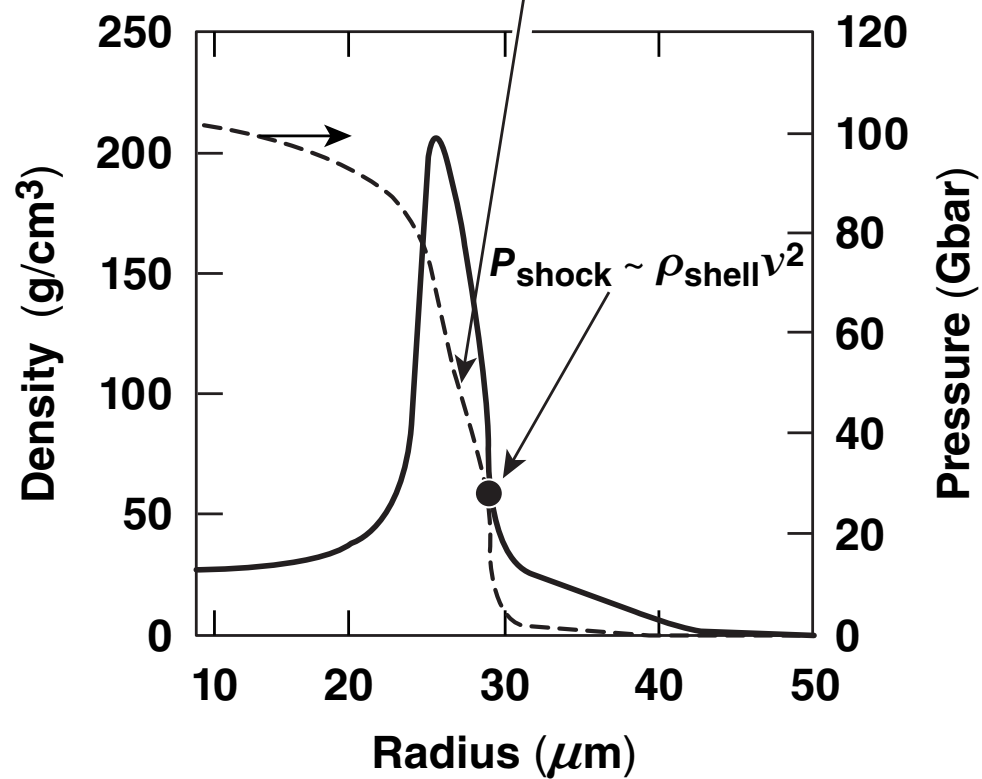


# Reduced shell density contributes to degradation in hot-spot compression

Shell decompression caused by instability growth at ablation front or preheat

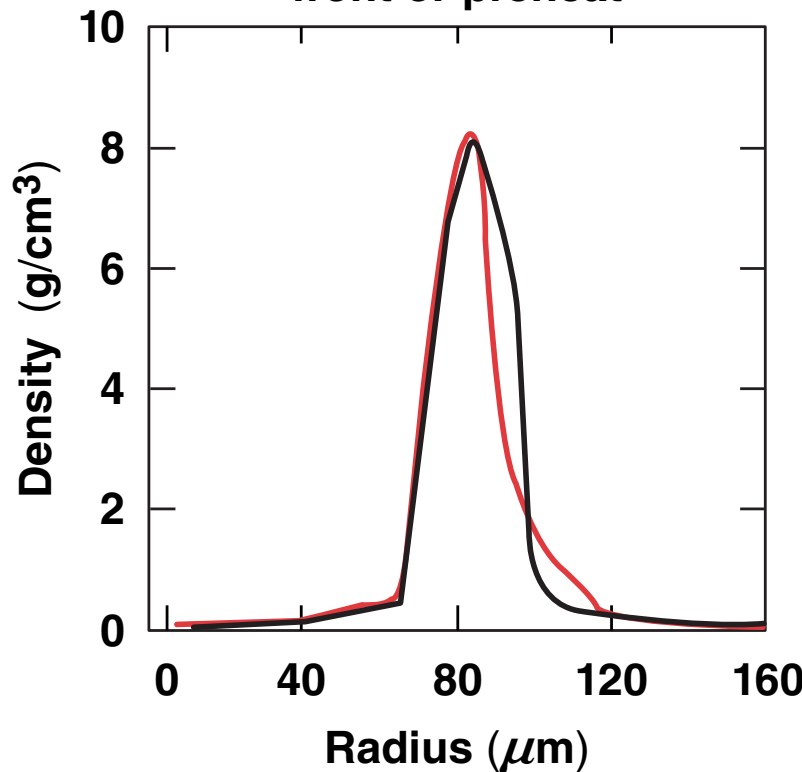


Pressure gradient stops the shell

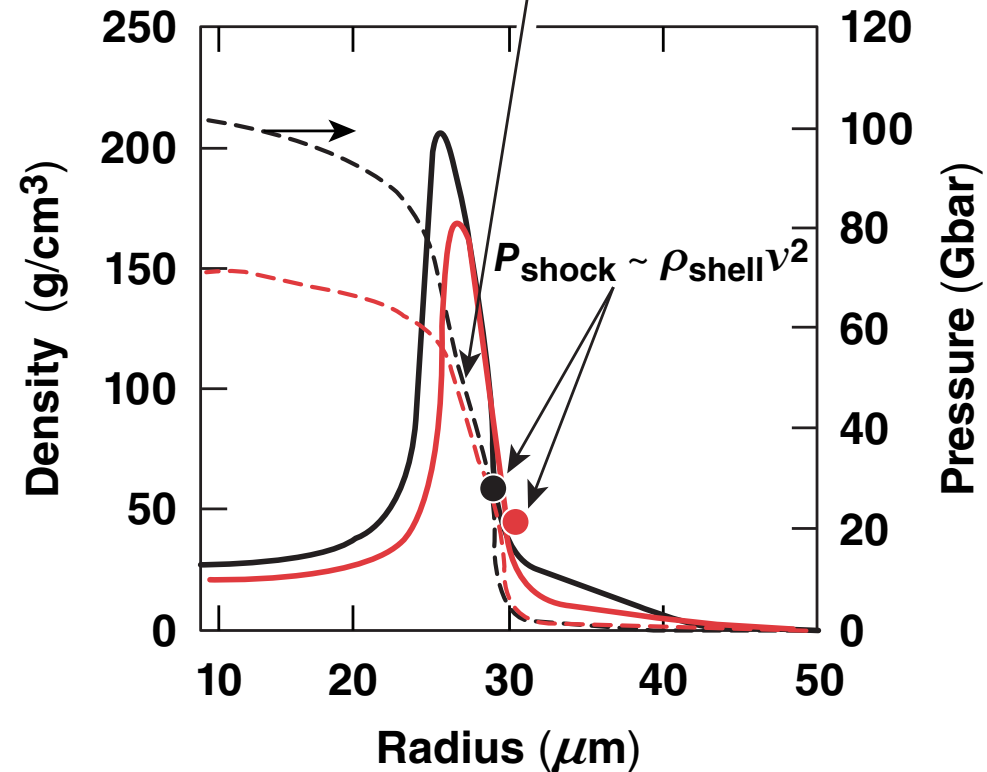


# Reduced shell density contributes to degradation in hot-spot compression

Shell decompression caused by instability growth at ablation front or preheat

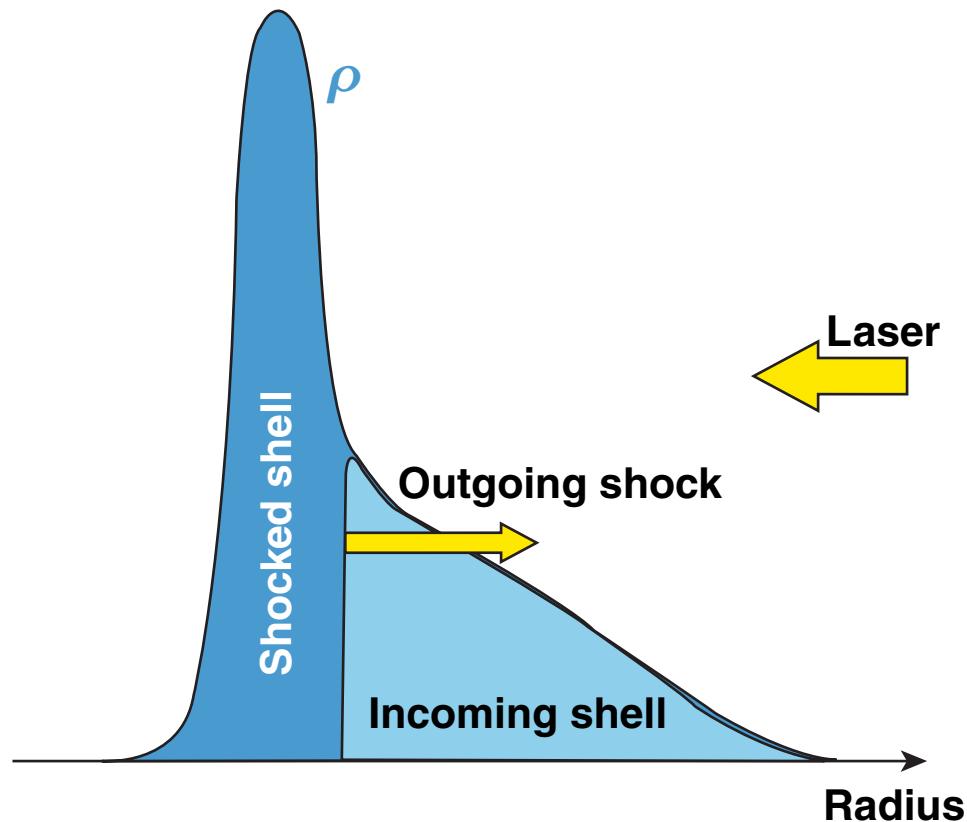


Pressure gradient stops the shell

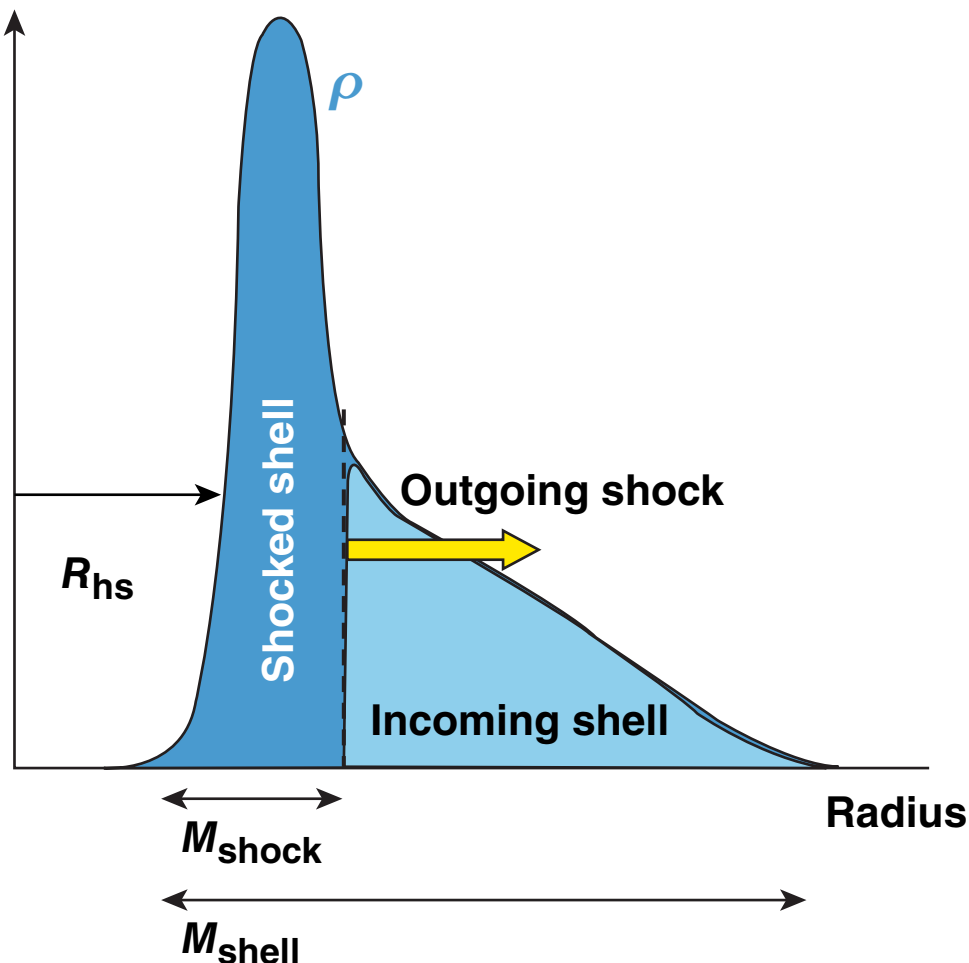


For smaller  $P_{\text{shock}}$ , lower  $P_{\text{hs}}$  stops the shell → larger stagnation hot-spot radius.

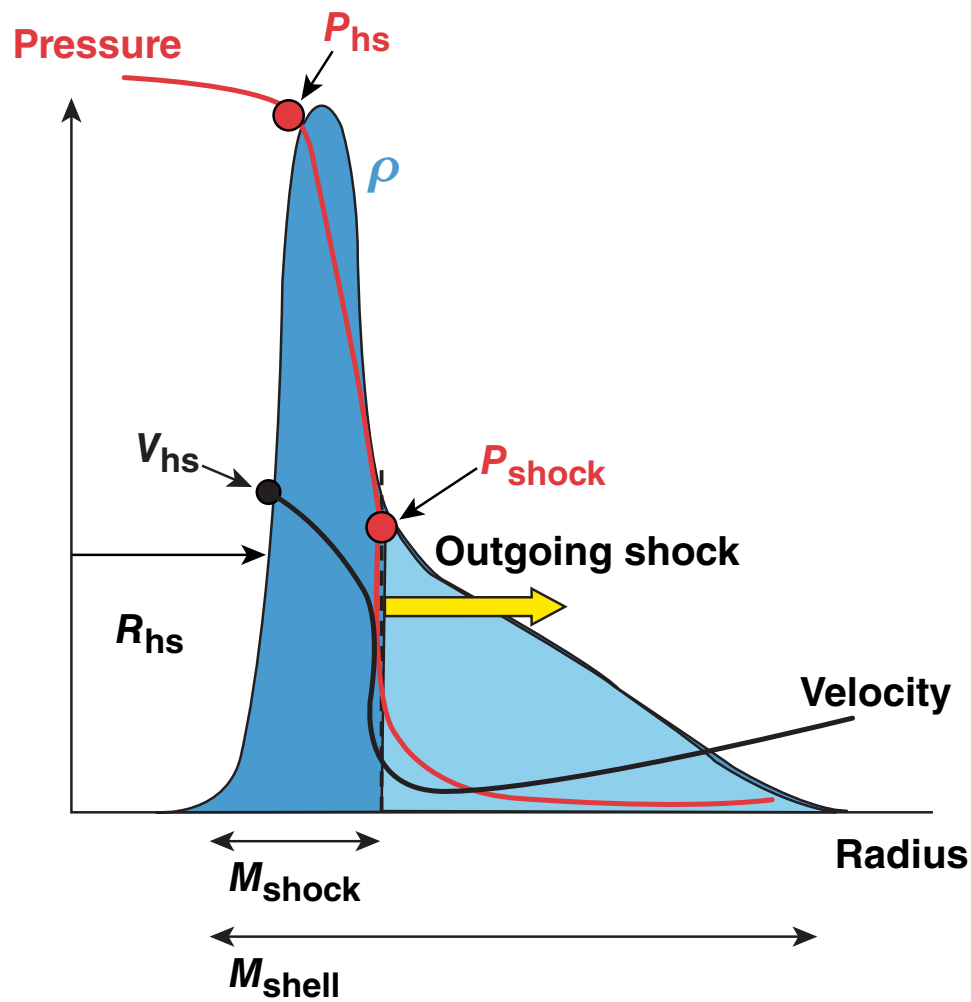
Target compression degradation caused by ablation-front mix depends on the fraction of shell mass overtaken by the shock at bang time



Target compression degradation caused by ablation-front mix depends on the fraction of shell mass overtaken by the shock at bang time

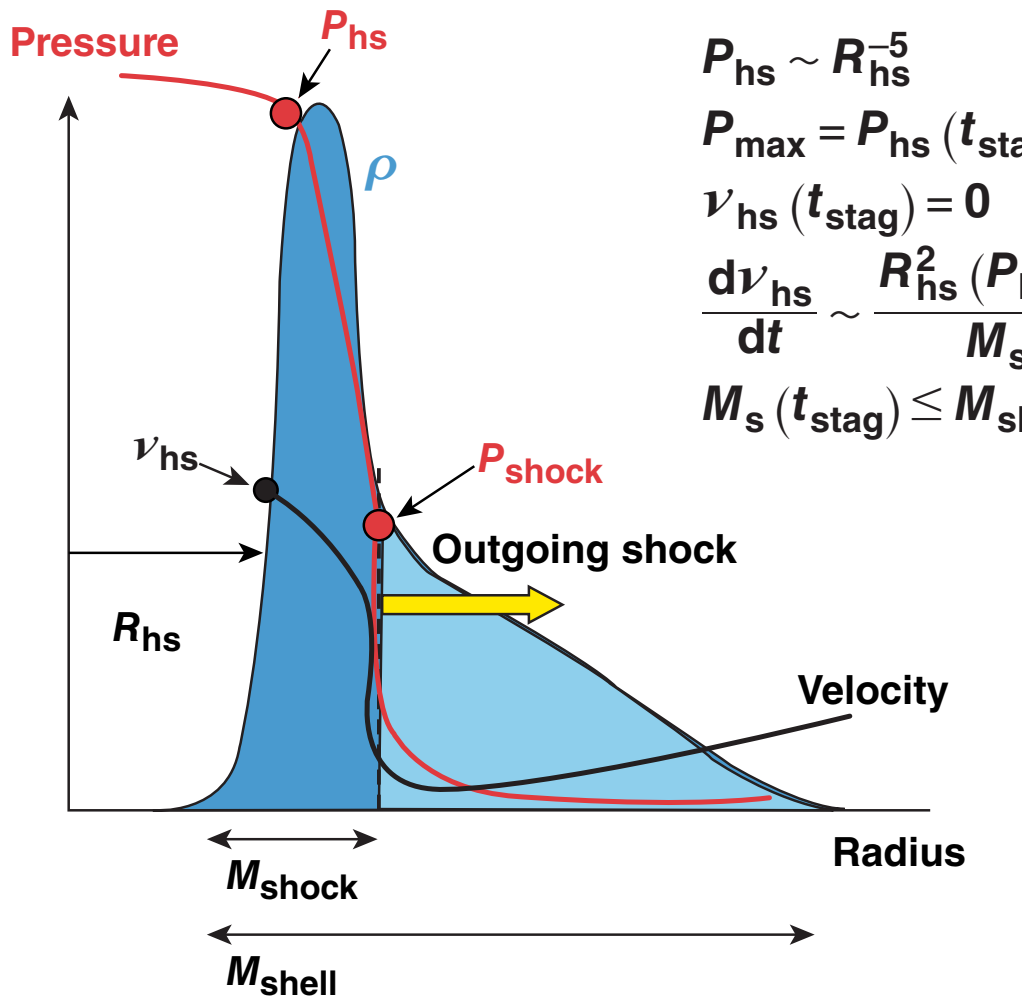


Target compression degradation caused by ablation-front mix depends on the fraction of shell mass overtaken by the shock at bang time



TC10993b

Target compression degradation caused by ablation-front mix depends on the fraction of shell mass overtaken by the shock at bang time



$$P_{hs} \sim R_{hs}^{-5}$$

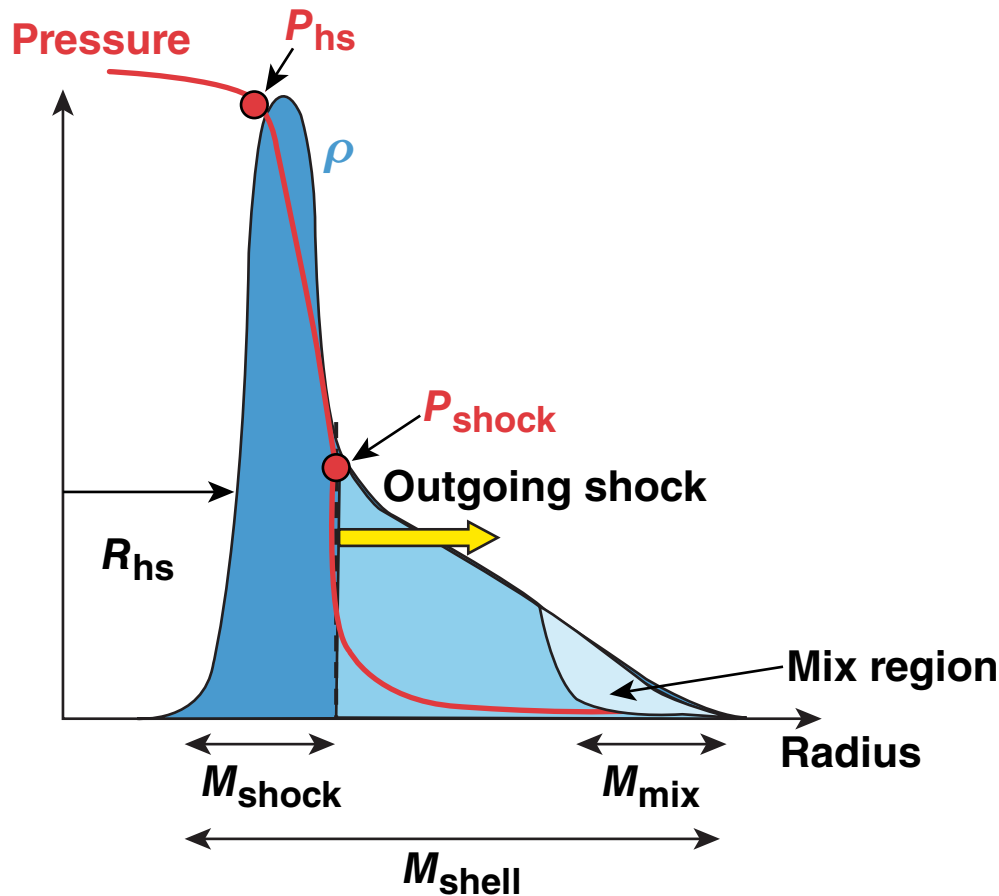
$$P_{\max} = P_{hs}(t_{stag})$$

$$v_{hs}(t_{stag}) = 0$$

$$\frac{dv_{hs}}{dt} \sim \frac{R_{hs}^2 (P_{hs} - P_{shock})}{M_{shock}(t)}$$

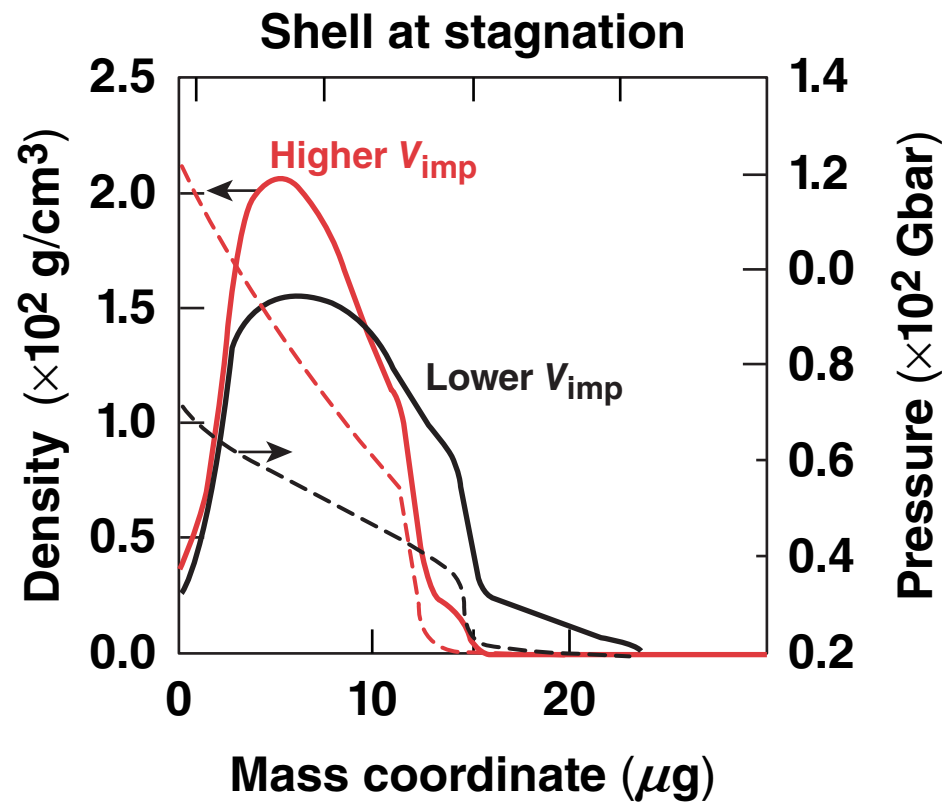
$$M_s(t_{stag}) \leq M_{shell}$$

Target compression degradation caused by ablation-front mix depends on the fraction of shell mass overtaken by the shock at bang time (continued)



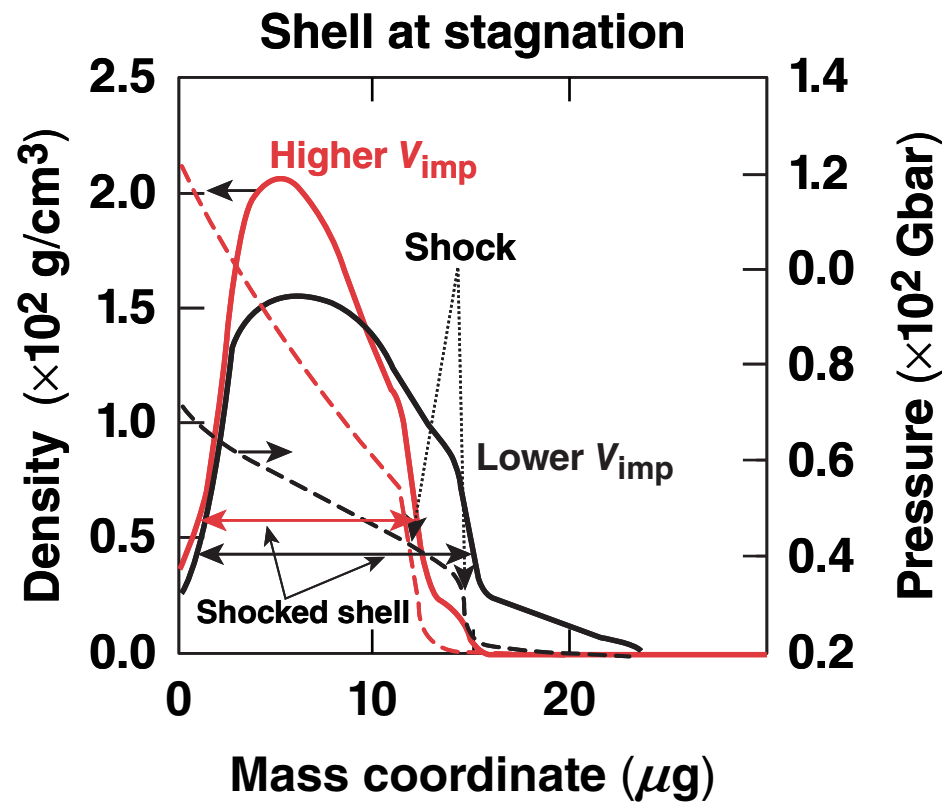
Target performance is not degraded if  $M_{mix} < M_{shell} - M_{shock}(t_{stag}) = M_{unshocked}$ .

# Shocked-shell fraction at stagnation depends on implosion velocity, adiabat, and drive pressure



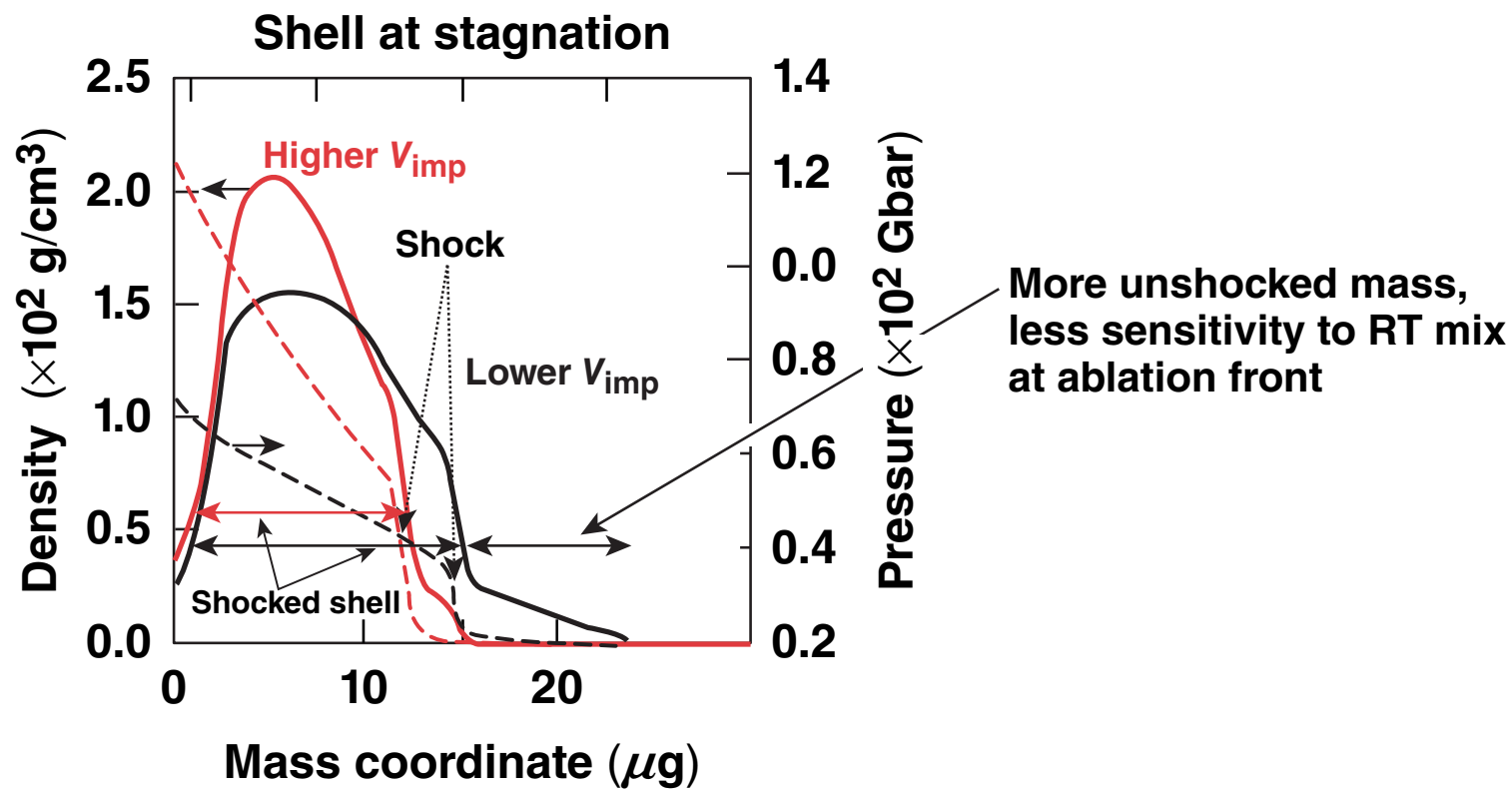
$$\frac{M_{\text{shock}}}{M_{\text{shell}}} \sim \frac{V_{\text{imp}}^{4/3}}{\alpha^{2/5} P_a^{4/15}}$$

# Shocked-shell fraction at stagnation depends on implosion velocity, adiabat, and drive pressure



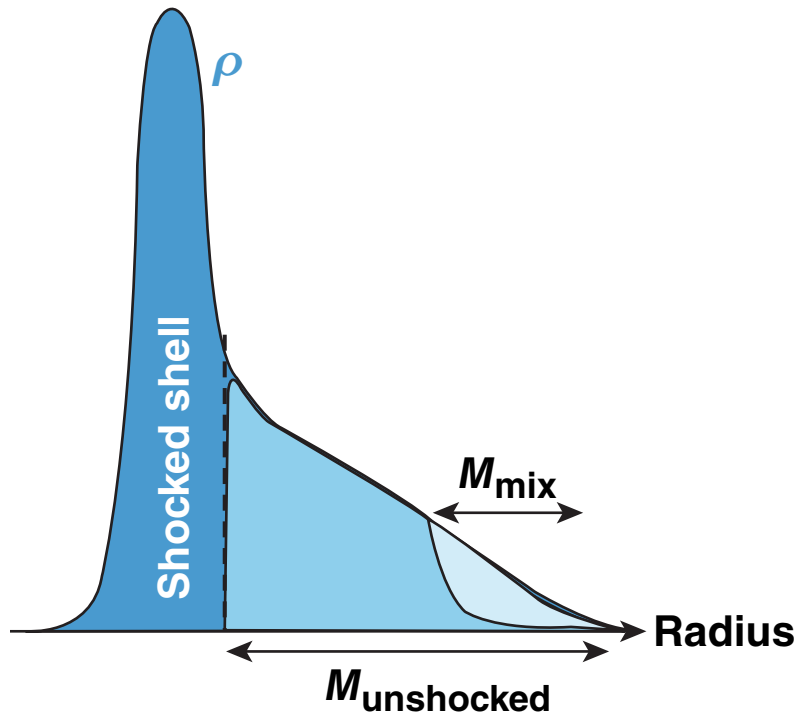
$$\frac{M_{\text{shock}}}{M_{\text{shell}}} \sim \frac{V_{\text{imp}}^{4/3}}{\alpha^{2/5} P_a^{4/15}}$$

# Shocked-shell fraction at stagnation depends on implosion velocity, adiabat, and drive pressure

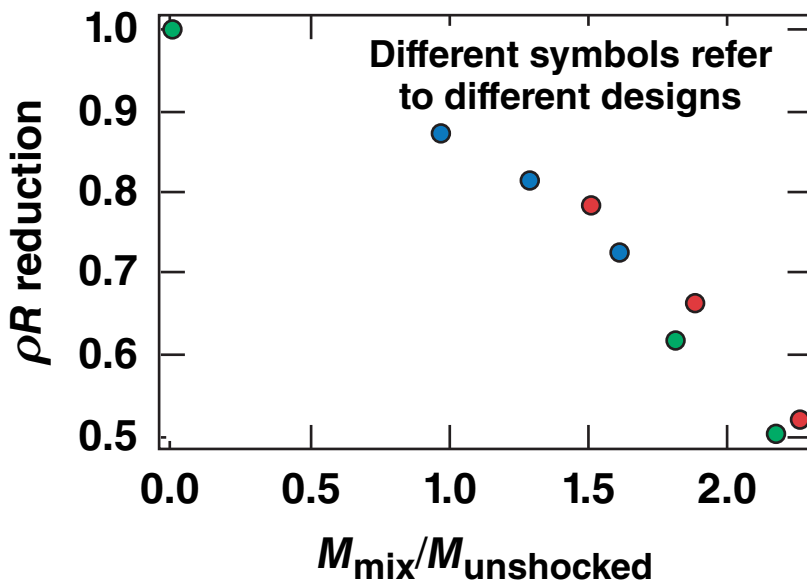


## Degradation Mechanisms

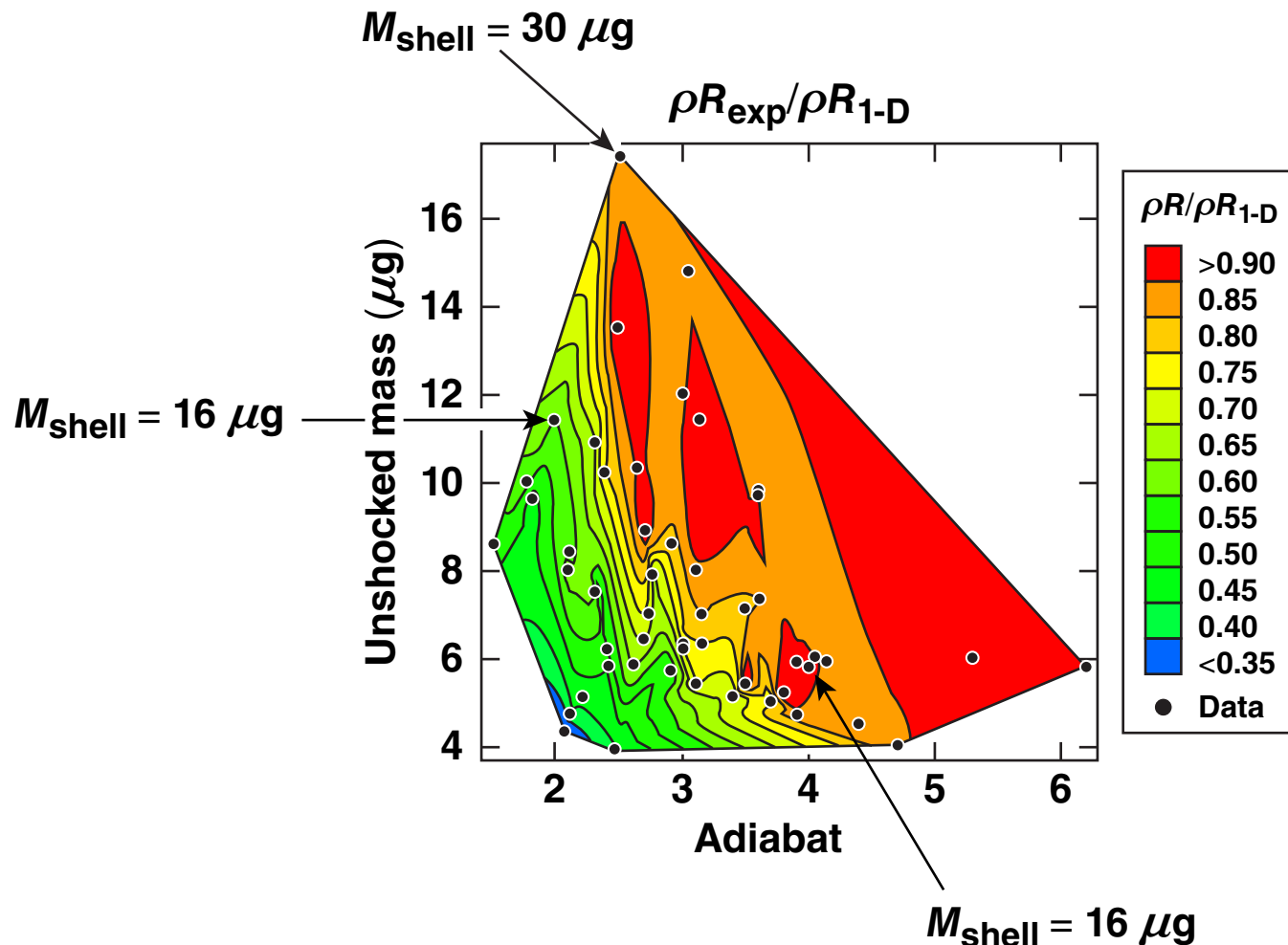
Reduction in peak areal density and pressure depends on the mass of the mix region relative to the unshocked mass



One-dimensional simulations with reduced density at the end of acceleration

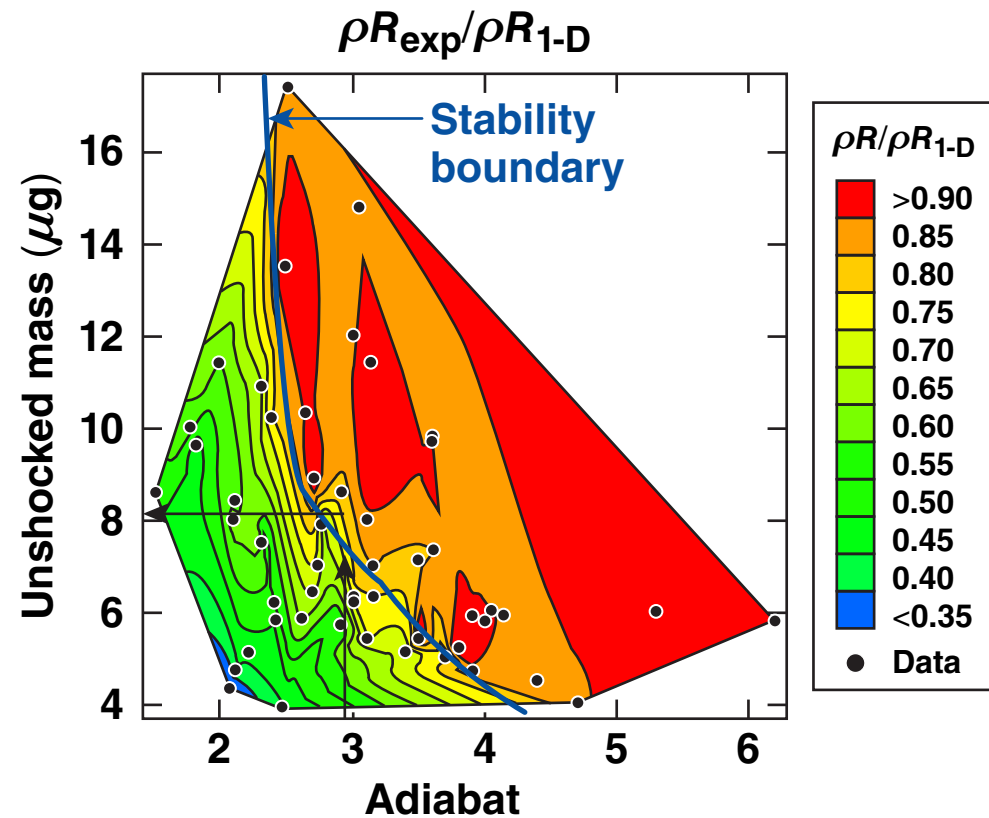


# Target compression degradation is a strong function of unshocked mass at peak neutron production



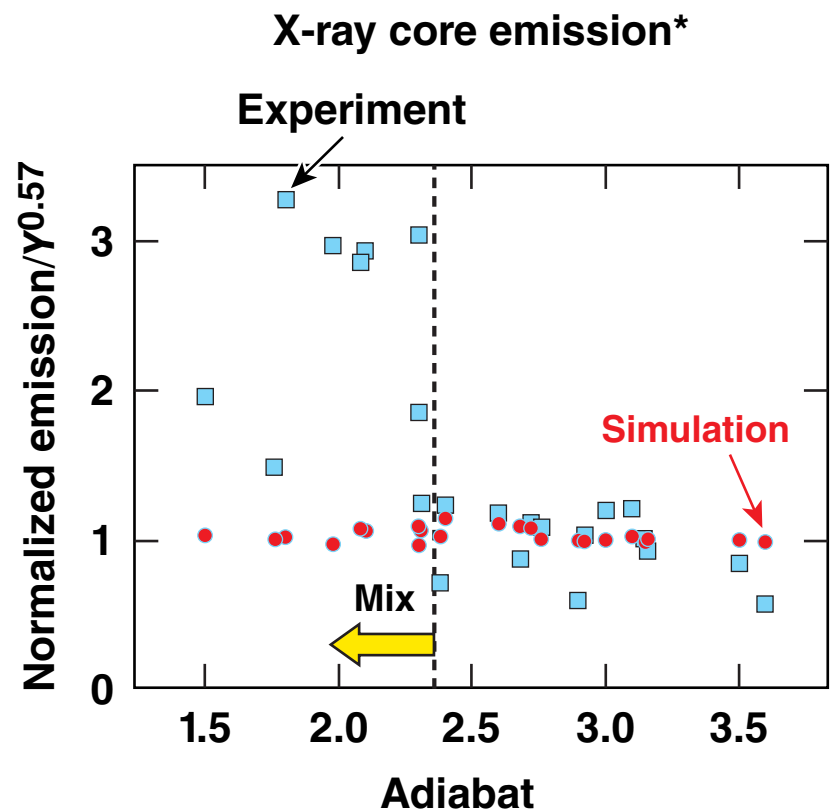
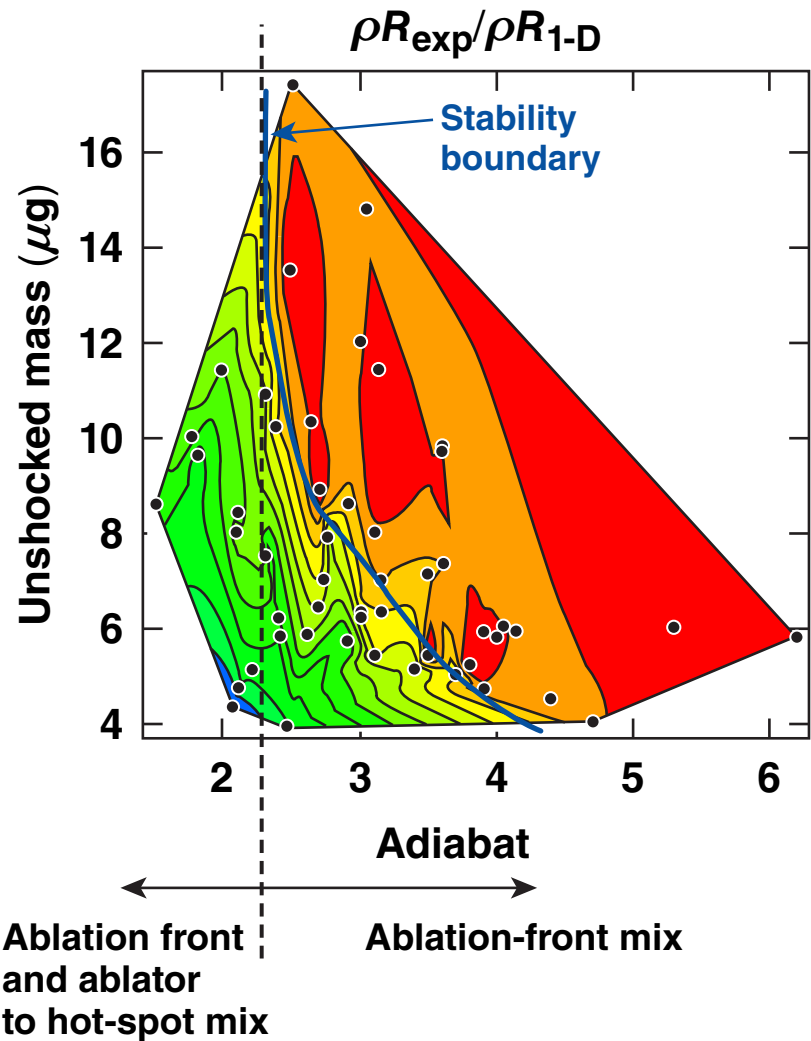
# Amount of RT mix at the ablation front can be inferred from the stability boundary

8  $\mu\text{g}$  of shell is mixed at the ablation front because of a RT growth

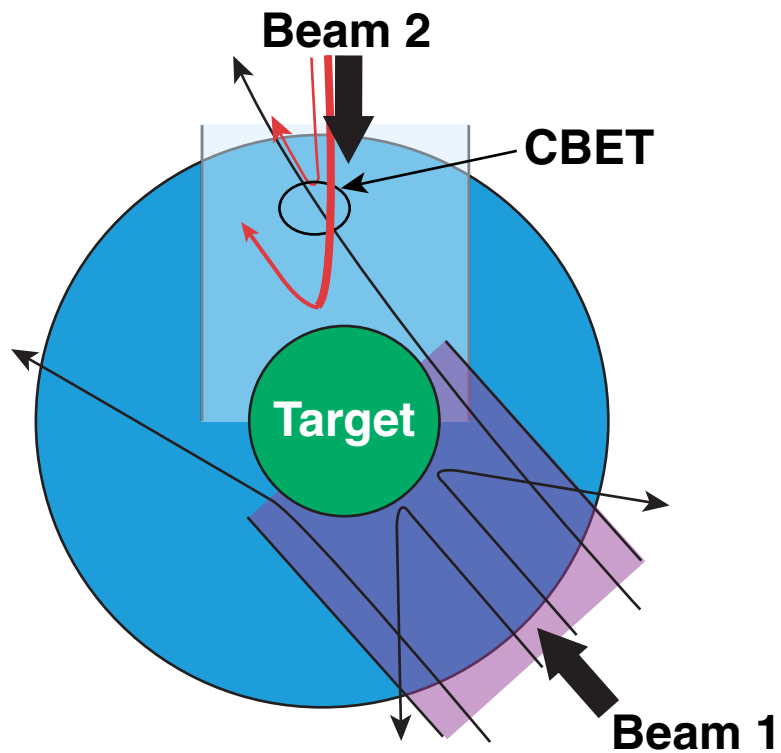


## Degradation Mechanisms

Significant mix of the ablator material into the hot-spot limits performance of  $\alpha < 2.5$  implosions



# Mitigating cross-beam energy transfer\* allows the shell and unshocked masses to be increased



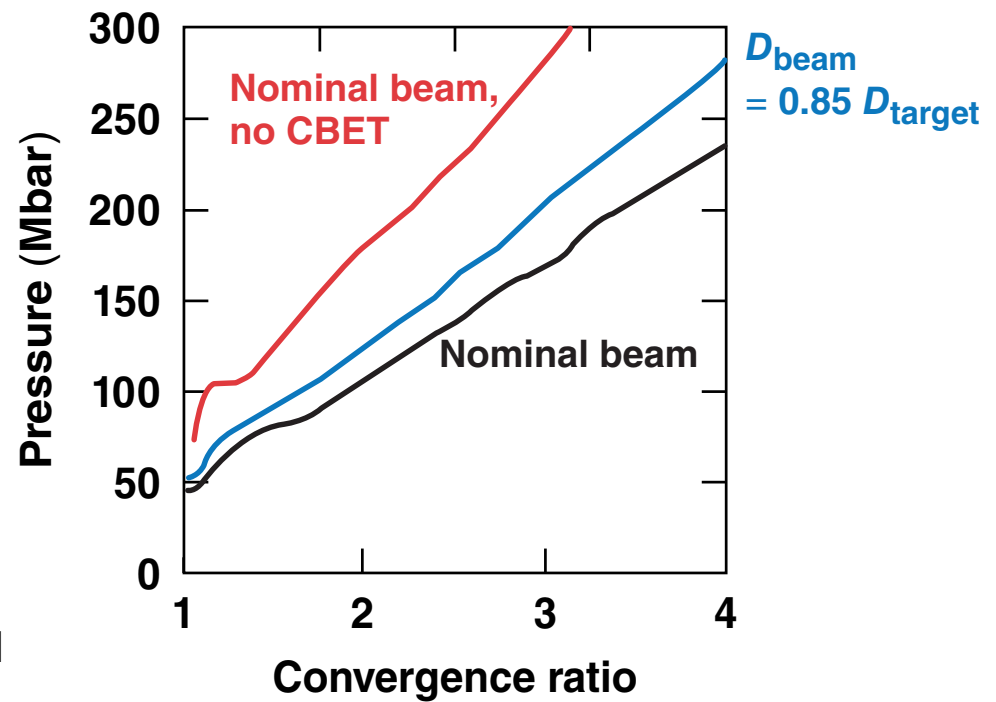
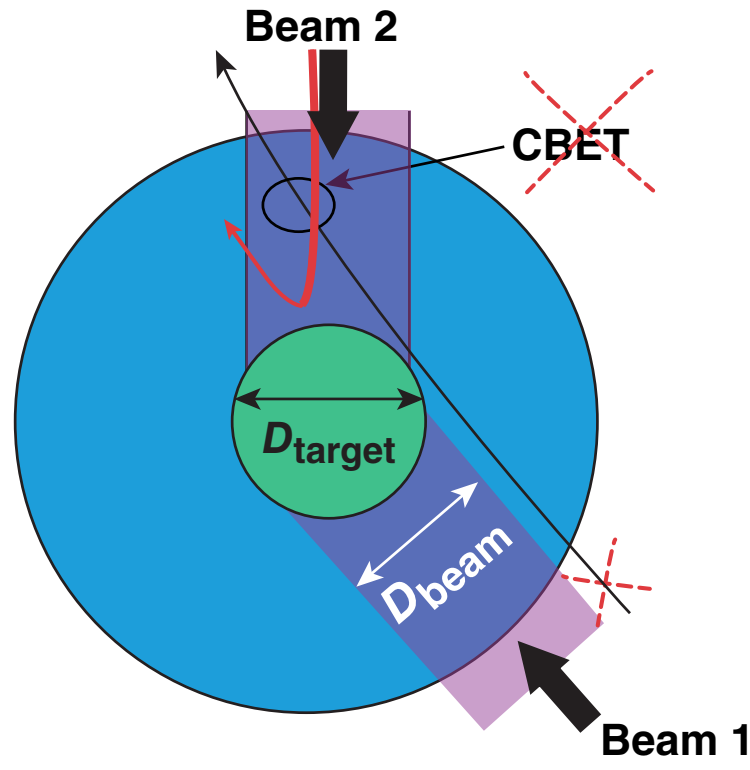
TC10997

\*I. V. Igumenshchev et al., Phys. Plasmas **17**, 122708 (2010).

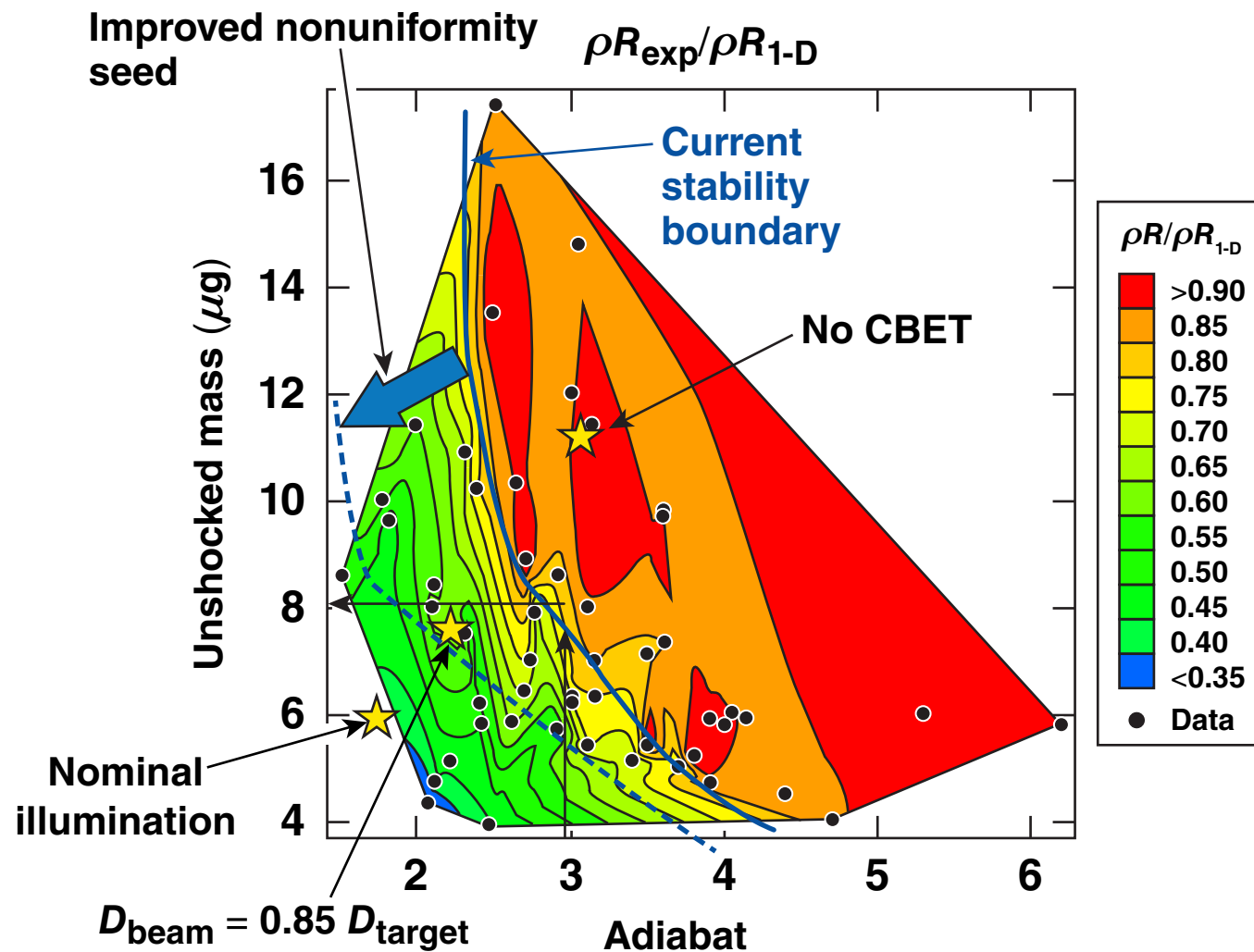
# Mitigating cross-beam energy transfer\* allows the shell and unshocked masses to increase



Using smaller beams at the main drive reduces CBET



# Mitigating CBET is required to demonstrate ignition hydrodynamic scaling on OMEGA



### ★ Hydro-equivalent designs

- Ignition hydrodynamic-equivalent OMEGA implosions require  $\rho R \sim 300 \text{ mg/cm}^2$  and  $V_{\text{imp}} \sim 3.7 \times 10^7 \text{ cm/s}$
- CBET mitigation strategies will be discussed in Michel, Myatt, and Froula's presentations\*

\*D. T. Michel et al., NO7.00002; J. F. Myatt, FR1.00001 (invited);  
D. H. Froula et al., CO7.00002, this conference.

# The perturbation degradation of OMEGA cryogenic implosions is understood in terms of unshocked shell mass at stagnation



- Yields in excess of  $3.4 \times 10^{13}$  [yield-over-clean (YOC) ~ 35%] and ion temperatures up to 4 keV were measured in cryogenic implosions with  $V_{\text{imp}} \sim 3.8 \times 10^7$  cm/s
- Performance degradation in moderate-adiabat ( $\alpha \sim 4$ ) implosions is fully understood by 2-D DRACO simulations
- Shells in lower-adiabat implosions ( $\alpha \sim 2.5$ ) break up during acceleration, leading to an increased hot-spot mass and reduced convergence
- The unshocked mass at peak compression determines the impact of the ablator mix

Improving shell stability and mitigating cross-beam energy transfer (CBET) are required to demonstrate ignition hydrodynamic scaling on OMEGA.